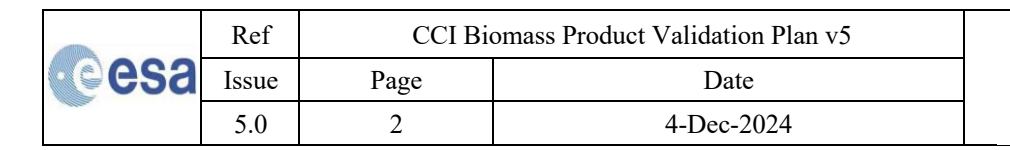
esa	Ref	CCI Bi	omass Product Validation Plan v5
	Issue	Page	Date
	5.0	1	4-Dec-2024



CCI BIOMASS Phase 2

PRODUCT VALIDATION PLAN PHASE 2 - YEAR 3 VERSION 5.0

DOCUMENT REF:	CCI_BIOMASS_PVP_V3
DELIVERABLE REF:	PVP
VERSION:	5.0
CREATION DATE:	2022-10-25
LAST MODIFIED	2025-01-07





Document Authorship

	NAME	FUNCTION	ORGANISATION	SIGNATU RE	DATE
PREPARED	Martin Herold	WP2000	GFZ		
PREPARED	Arnan Araza	WP2000	GFZ/WUR		
PREPARED	Jerome Chave	WP2000	CNRS		
PREPARED	Nicolas Labrière	WP2000	CNRS		
PREPARED	Richard Lucas	Project Manager	Aberystwyth University		
Prepared					
VERIFIED	H.Friendship-Kay	Project Coordinator	Aberystwyth University		
VERIFIED	S. Quegan	Science Leader	Sheffield University		
Approved					

Document Distribution

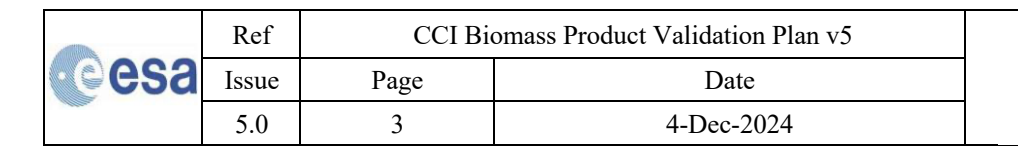
ORGANISATION	Name	Quantity
ESA	Frank Seifert	

Document History

VERSION	DATE	DESCRIPTION	APPROVED
4.0	25-10-2024	First draft version	
5.0	04-12-2024	Revised version	

Document Change Record (from Year 1 to Year 2)

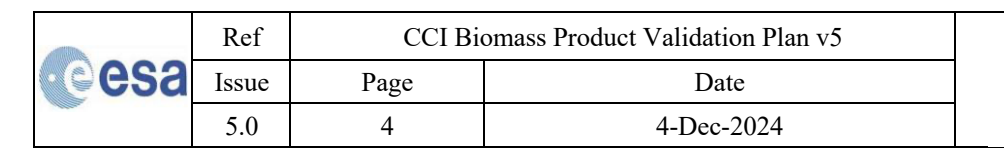
VERSION	DATE	DESCRIPTION	APPROVED
5.0	Febr. 2023	Version one of Product validation plan of phase 2 (ver. 4.0)	





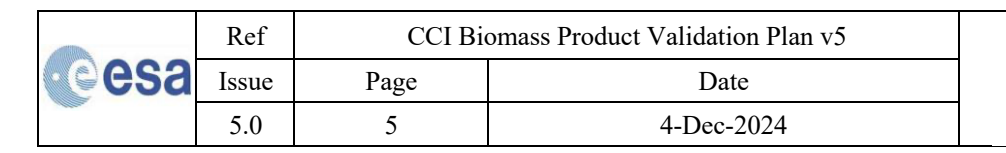
CONTENTS

Li	st of to	bles	5
Li	st of fi	gures	6
S	ymbols	and acronyms	7
1.	Intr	oduction	9
2.	Con	cepts	11
	2.1.	Definitions	11
	2.2.	Statistics	11
3.	Date	abase compilation for biomass stocks	13
	3.1.	Sources of reference data	13
	3.2.	Sampling design	13
	3.3.	Tiers of plot data and other in situ data	14
	3.4.	Data harmonization	
4.	Date	abase compilation for biomass changes	
	4.1.	Sources of reference data	
	4.2.	Data processing and harmonization	18
	4.3.	Characteristics of reference data	
5.	_	o-plot comparisons	
	5.1.	Assumptions	
	5.2.	Descriptive analyses	
	5.3.	Stratification and spatial aggregation for stocks	
	5.3.1		
	5.3.2		
	5.4.	Spatial aggregation for AGB change	23
6.	Spa	tial uncertainty modelling for biomass	24
	6.1.	Definition of the error model	24
	6.2.	Identification of the error model	
	6.2.1 6.2.2		
	6.2.3	·	
	6.3.	Model-based prediction	26
	6.3.1		
	6.3.2	5 5	
	6.3.3 6.3.4		
7.		o inter-comparison	
	7.1.	Stability of AGB _{map} – AGB _{ref} among CCI Biomass products	28
	7.2.	Comparison of CCI Biomass maps with other AGB products	





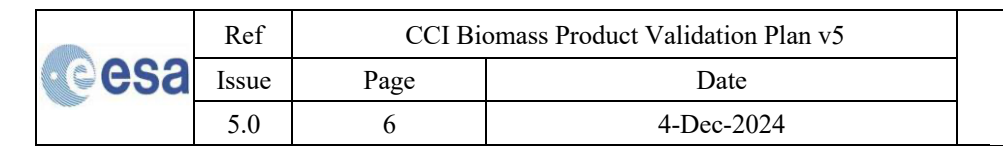
8.	Expert assessment	<i>32</i>
Ref	erences	34
APF	PENDIX 1	37
APF	PENDIX 2	42





LIST OF TABLES

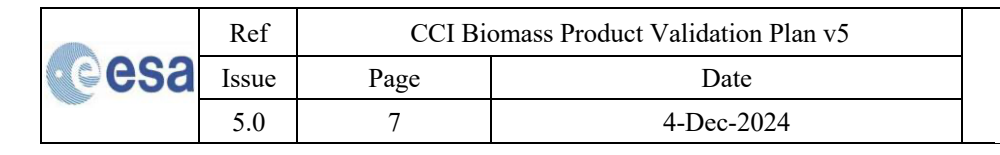
Table 1. Statistics used in this PVP.	12
Table 2. Details of the \triangle AGB map-reference data comparisons and the selection of grid cells.	23
Table 3. Estimation methods for the parameters of the uncertainty model.	25





LIST OF FIGURES

Figure 1. Validation objectives (left) and derived validation activities (right).	9
Figure 2. Geographical locations of plots and footprints (CoFor and LiDAR) of the reference datasets collected up to January 2021. This figure will be updated in the next PVIR.	d 16
Figure 3. Overview of data harmonization steps.	17
Figure 4. Coverage of the reference data per major ecological zone (a) and the map of the selected reference data (b). The reference data are already quality-filtered.	9 19
Figure 5. Distributions according to NFI and LiDAR data for the five aggregation levels.	20
Figure 6. Example of a AGB_{map} - AGB_{ref} comparison plot taken from de Bruin et al. (2020b).	21
Figure 7. Example of AGB residuals between harmonized Tier 1–3 plot data and mapped AGB at 0.1° cell leve for each combination of map reference years. The red dashed line is the 1:1 line.	el 29
Figure 8. Example comparison of different global biomass maps against harmonized plot data.	31
Figure 9 Wales (left) and Japan (right) country cases of validating the CCI man through the MAAP	33





SYMBOLS AND ACRONYMS

AGB Above-ground biomass density (in general) \triangle AGB Above-ground biomass change (in general)

AGB_{map} Above-ground biomass density according to the map

AGB_{plot} In situ above-ground biomass density

AGB_{ref} AGB_{plot}, corrected for inventory date and if footprint < 1 ha corrected for forest fraction

AGB* True above-ground biomass density

ALS Aerial Laser Scanning
BGB Below-ground biomass
CCI Climate Change Initiative

CEOS Committee on Earth Observation Satellites

CI Confidence Interval

CoFor Congo basin Forests AGB dataset (Ploton et al., 2020)

DRC Democratic Republic of the Congo

ECV Essential Climate Variables
ESA European Space Agency

FAO Food and Agriculture Organisation
FRA Forest Resources Assessment

IPCC Intergovernmental Panel on Climate Change

LiDAR Light Detection And Ranging
LPV Land Product Validation

MAAP Multi-mission Algorithm Analysis Platform

MSE Mean Squared Error

NEON National Ecological Observatory Network

NFI National Forest Inventory

PI Prediction Interval

PVIR Product Validation and Intercomparison Report

PVP Product Validation Plan

RMSD Root Mean Squared Difference SAR Synthetic Aperture Radar

SD Standard Deviation

SLB Sustainable Landscape Brazil

TERN Terrestrial Ecosystem Research Network

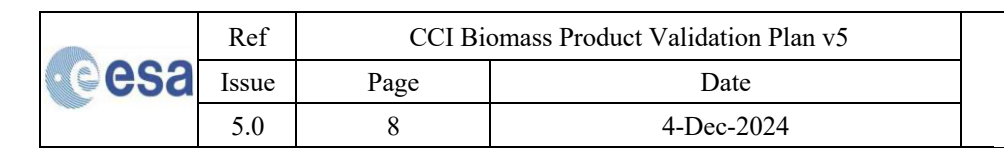
Var Variance

 $\gamma_{AGB}(h)$ Variogram model of AGB with a spatial support matching the smallest plot size used our

analyses

 $\gamma_{M}(h)$ Variogram model of the residuals between AGB_{map} and AGB_{ref}, with a spatial support matching

the map pixels.





esa	Ref	CCI Bio	omass Product Validation Plan v5	
	Issue	Page	Date	
	5.0	9	4-Dec-2024	



1. Introduction

This Product Validation Plan (PVP) aims to provide a common framework for assessing and reporting the accuracy of the European Space Agency's (ESA) Climate Change Initiative (CCI) Biomass products, namely the various global above-ground biomass (AGB) maps as well as the corresponding uncertainty layers, and to assess user appreciation of these products. Elaboration of the plan and the forthcoming validation itself run in parallel with ongoing Committee on Earth Observation Satellites (CEOS) cal/val development, which provides opportunities for co-creation of the CEOS cal/val procedure. We further build on results of the GlobBiomass project (Avitabile et al. 2015, Rozendaal et al. 2017) and the CCI Biomass Phase 1 project and the related validation efforts. In fact, the annual map validation uses the same framework as in Phase 1. In addition, there is a focus on exploring options towards validation of AGB change obtained through comparison of the global AGB maps between time-separated periods (years to decades) and exploring options for direct and independent biomass change accuracy analysis. The framework consists of five main activities that jointly lead to the achievement of the validation objectives, as shown in Figure 1.

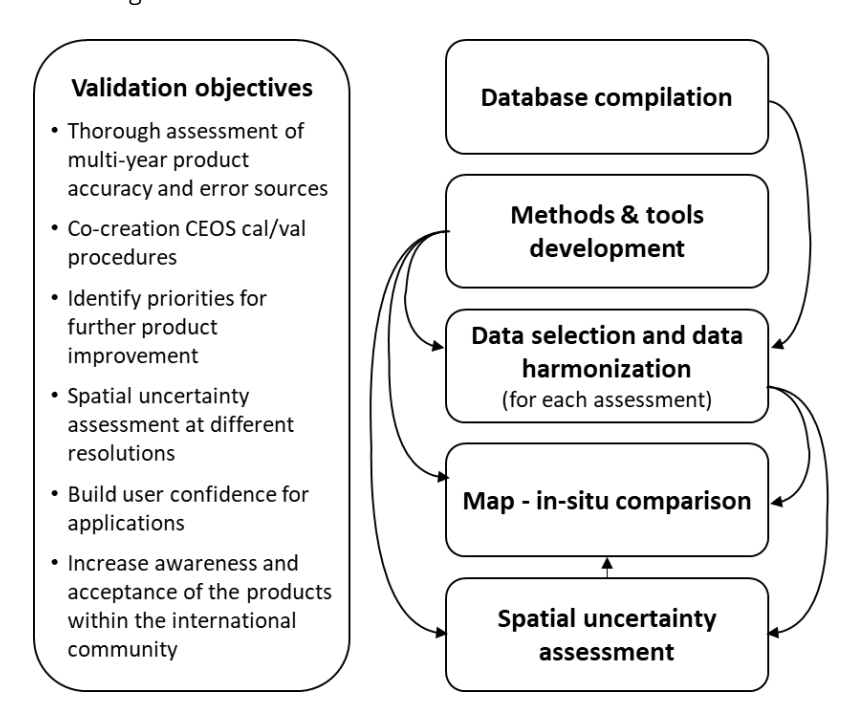
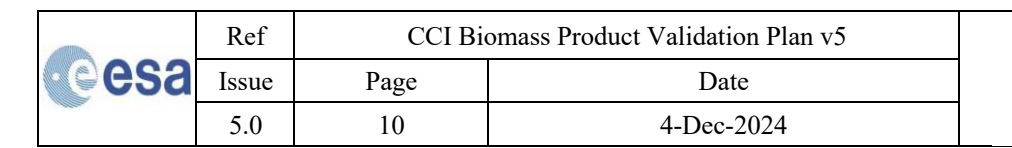


Figure 1. Validation objectives (left) and derived validation activities (right).

As with its predecessors from CCI Biomass Phase 1 (de Bruin et al. 2019a, de Bruin et al. 2020a), this Product Validation Plan is developed in line with the new CEOS Land Product Validation (LPV) protocol for biomass for space calibration and validation. The new CEOS protocol contains a dedicated section about using existing *in situ* data as a reference for the validation of larger area AGB maps, assuming they are properly screened, processed and harmonized, to allow for comparison with large area AGB map predictions. It is recognized that different users, such as national inventory experts, global climate modelers, local project implementers, etc., all have specific needs when it comes to biomass estimation and uncertainty assessment with respect to spatial resolution, geographic extent, timing, thematic content and definitions, and type and standards of uncertainty reporting. The CCI Biomass project and its climate users are also interested in spatially explicit assessments of map precision and map bias in addition to the more standard accuracy analysis undertaken for AGB map validation exercises. This requires an effort to include a large number of *in situ* data sources covering all major geographical





regions and forest types (top box on the right of Figure 1). The main data sources of forest biomass information include National Forest Inventories (NFIs), research forest plot networks and operational monitoring stations established for forestry, ecology or environmental purposes, including those using local Light Detection and Ranging (LiDAR) observations from which AGB and ideally associated estimates of uncertainty have been estimated.

The second box from the top at the right-hand side of Figure 1 indicates that a common set of data harmonization and analysis methods and tools is developed and used. To support wider use, these are provided in the form of an R-package that allows the climate change community (both within and outside the project) to assess maps of AGB based on their own reference data, without the need to upload those data to an external database.

The centre box at the right-hand side of Figure 1 refers to $in\ situ$ data selection from the database, based on a set of pre-defined quality criteria. The box further denotes data harmonization to adjust for any partial forest cover within map pixels and allowable (< 10 years) temporal mismatches between the map reference year and the $in\ situ$ AGB inventory date.

Map-plot comparison (fourth box from the top in Figure 1) concerns statistical assessment of differences between map and *in situ* estimates of AGB over reference AGB ranges. The assessments are performed at the map pixel level, as well as spatially aggregated over larger pixel blocks. They are also differentiated over ecoregions, realms¹ and slope and aspect classes which have been found to affect AGB retrieval from satellite data (e.g., Réjou-Méchain et al. 2019). The aims of the map-plot comparisons are to assess whether the biomass map satisfies design specifications (relative error of less than 20% where AGB exceeds 50 Mg/ha) and to provide map producers with information on how and where to improve their products. It is important to realize that the reference data are also estimates and therefore affected by errors that should be taken into account when using them in the map-plot comparisons (Réjou-Méchain et al. 2017, Réjou-Méchain et al. 2019). This is indicated by the short upward arrow in the bottom-right of Figure 1.

These essential steps for validation of AGB maps also relate to the potential assessment of AGB changes. With this PVP, we provide the first steps and concepts towards an AGB change validation framework. This is in response to the proliferation of different approaches being developed to estimate AGB change over larger areas including from AGB between different time-separated maps at different spatial resolutions. We explain that there are different reference data sources and to what extent they are available and suitable for any future AGB change validation exercises.

During the CCI Biomass User Workshops and later communications, the climate, carbon cycle and REDD+ communities expressed the need for unbiased biomass estimates accompanied by spatially explicit uncertainty information at spatial resolutions ranging from the 1 ha resolution of CCI Biomass up to 0.5 or even 1-degree cells (for climate modelling) or countries (for REDD+) (Quegan and Ciais 2018 and CCI Biomass Phase 2 User Requirements Document). Hence, CCI Biomass product validation should explicitly address estimation of systematic deviations and random differences between reference and map biomass and uncertainty assessment at different spatial aggregation levels. This is indicated by the box at the bottom-right of Figure 1.

Details of the approaches are provided in later chapters of this validation plan.

.

¹ Biogeographic realms are large spatial regions within which ecosystems share a broadly similar biological evolutionary history. Eight terrestrial biogeographic realms are typically recognized, corresponding roughly to continents. See Dinerstein, et al. (2017).

esa	Ref	CCI Bio	omass Product Validation Plan v5
	Issue	Page	Date
	5.0	11	4-Dec-2024



2. Concepts

2.1. Definitions

Accuracy is only occasionally used in this document to *qualitatively* refer to both random and systematic error. This use of the term is in line with the ISO 5725 definition of accuracy.

Bias expresses the degree to which the expected value of an estimator differs from the true value of the quantitative parameter being estimated.

Error. For a continuous variable such as AGB, error is defined as the difference between our representation of reality (e.g., a mapped AGB value) and reality (e.g., a true AGB value). We can only know error at some locations, if at all, because we rely on scarce reference values (e.g., from plots) which themselves are estimates of reality. Therefore, we will often refer to *differences* or *residuals* between mapped AGB values and reference AGB.

Precision denotes the dispersion of random errors; it is expressed by measures of statistical variability such as variance and standard deviation.

Stability. According to the World Meteorological Organization (2011), stability is the extent to which the error of a product remains constant over a longer period of time.

Systematic deviation of biomass refers to a systematic difference between predicted biomass (on the map) and reference biomass obtained from plot data. Only if plot data (which themselves are estimates) are unbiased, systematic deviation would equal bias. We assume the plot data to be unbiased.

Uncertainty is a *quantitative* description of error: we are aware that our representation differs from reality, but we are only able to model the distribution of error (expressed by a probability distribution) or, in many cases, just some statistic, such as standard deviation of the error, rather than the error itself. This is a common situation, because if we knew error, we would simply correct for it and reduce the error to zero.

2.2. Statistics

Table 1 lists the statistics used in this PVP, as well as their definitions, where E is the expected value, Z denotes a random variable, μ is the mean of Z, Y is a vector of n reference values, \hat{Y} is a vector of n predicted values (i.e., CCI Biomass predictions), and h denotes a distance between two locations x.

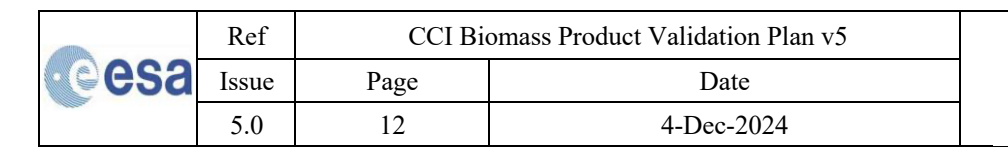




Table 1. Statistics used in this PVP.

Acronym	Name	Description	Definition
Var	Variance	Measure of spread of a random variable (<i>Z</i>)	$Var(Z) = E[(Z - \mu)^2]$
SD	Standard deviation	Measure of spread of a random variable; square root of the variance	$SD(Z) = \sqrt{Var(Z)}$
d_i	Observed difference	Difference between a predicted value, \hat{y}_i and a reference value, y_i , where i refers to a particular instance, e.g., a location.	$d_i = \hat{y}_i - y_i$
MD	Mean difference	Average difference between reference values and predicted values	$MD = \frac{1}{n} \sum_{i=1}^{n} d_i$
MSD	Mean squared difference	Average squared difference between reference values and predicted values	$MSD = \frac{1}{n} \sum_{i=1}^{n} d_i^2$
RMSD	Root mean squared difference	Square root of MSD	$RMSD = \sqrt{MSD}$
CI	Confidence interval	Measure of uncertainty associated with a sample population estimate (e.g., μ); intervals covering individual observations commonly referred to as prediction intervals (see below).	Estimated range of values likely to include an unknown population property.
PI	Prediction interval	Measure of uncertainty associated with the prediction of single observations	Estimated range in which a new observation falls, with a certain probability, given an existing model
$\gamma(h)$	(Semi)variogram	Function describing the degree of spatial dependence of a spatial random field, where <i>x</i> is a spatial position and <i>h</i> is a distance lag	$\gamma(h) = \frac{1}{2} Var[Z(x) - Z(x+h)]$
$\sigma_{i,j}$	Spatial covariance	Element of the spatial covariance matrix, Σ , where i and j (1 n) refer to pixels within a spatial unit	$\sigma_{i,j} = \mathbb{E}[Z(x) - \mathbb{E}(Z(x))] \\ \cdot \mathbb{E}[Z(x+h) \\ - \mathbb{E}(Z(x+h))],$

	Ref	CCI Bio	omass Product Validation Plan v5	
esa	Issue	Page	Date	ć
	5.0	13	4-Dec-2024	



3. Database compilation for biomass stocks

3.1. Sources of reference data

Building upon the GlobBiomass reference database (Rozendaal et al. 2017), an extensive dataset of forest *in situ* data across the world has been acquired for the purpose of the validation (see Appendix 1, Figure 2). Plots included in the database undergo a series of quality checks (see below). *In situ* forest data were not used for calibrating the CCI Biomass AGB map to guarantee full independence from the production process and because the project's AGB map processing chain does not rely on such a calibration procedure.

The following *in situ* data selection criteria are used for CCI Biomass product validation. *In situ* data need:

- A proper citable reference source and metadata to assess the procedures and quality of biomass (AGB but also below-ground biomass (BGB) when collected) estimation.
- Precise coordinates (4-6 decimals for coordinates in decimal degrees).
- A census date within ten years from the reference year of the AGB map to avoid temporal inconsistency with the assessed maps.
- Measurements of all trees of diameter ≥ 10 cm (or less) included in the estimates.
- Sites that were not deforested between the year of the inventory and the reference year of the CCI Biomass AGB map (i.e., 2010 and 2017-2020). The latter assessment is based on the 2021 forest loss layer of the Hansen dataset (Hansen et al., 2013).
- LiDAR-derived AGB or other indirect AGB data should be accompanied by estimates of the standard deviation of AGB error.

Note that the current data agreements will have to be renewed, and new agreements established.

Alternatively, reference data coming from harmonized and aggregated reference data described above can be used for validation. This AGB reference dataset ("AGBref") comes at different spatial aggregates and epochs, is published as a scientific data and can be downloaded from Zenodo (under preparation).

3.2. Sampling design

We primarily rely on AGB *in situ* data that are not specifically produced for validation purposes but that are rather collected within the context of NFIs and other efforts at local to regional scale. This has several consequences, which are summarised as follows:

- The populations of the CCI Biomass products and those of the inventories differ. CCI Biomass concerns forest AGB over the entire globe (including areas without forest), whereas forest inventories typically only concern forested areas within countries or regions. Moreover, large portions of the world including Southeast Asia, large parts of Africa, the dry tropics and Siberia have very little or no *in situ* data (see Figure 2).
- The sampling frames are different: CCI Biomass concerns mean forest AGB density estimates discretised in ~100m × 100 m pixels (including non-forested areas) while the inventories employ

	Ref	CCI Bi	omass Product Validation Plan v5	
esa	Issue	Page	Date	
	5.0	14	4-Dec-2024	



non-uniformly sized and typically small plots (on average 0.15 ha for the AGB plot data referred to in Appendix 1) within forested areas.

- Regionally, the AGB plot locations may have been chosen by probability sampling but large areas
 of the world are not included in the AGB plot sample (see first bullet). That is because in these
 areas, there are no national forest inventories or because institutions or authorities are unwilling
 to share inventory data.
- The wide variety of sampling designs included in the AGB *in situ* dataset produces a complex amalgamated sample.

Given the above, our approach is to consider the AGB *in situ* data with its mix of plot sizes or footprints and local sampling designs as an opportunistic sample (also referred to as an *ad hoc* sample by other authors). Such sampling invalidates conventional statistical inference methods unless particular assumptions are made (see section 5.1).

Additionally, a model-based approach is adopted here, with the model parameters estimated from the *in situ* data along with other data sources (see section 6.2).

3.3. Tiers of plot data and other in situ data

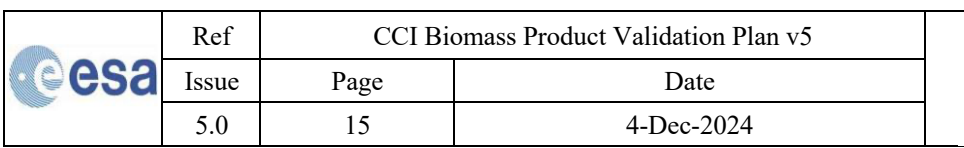
The contributions of AGB measurement error and within-pixel sampling error (see section 6.1) are known to be largest for small plots, including those associated with NFIs, whereas detailed measurements of all trees within large plots deliver higher quality AGB data (Réjou-Méchain et al. 2014, Réjou-Méchain et al. 2019).

A straightforward approach for taking into account expected differences in the accuracy of plot data is to adopt a tiered approach comprising (Tier 1) small plots (\leq 0.6 ha) including NFI data, (Tier 2) larger plots with sizes in the range 0.9-3 ha, and (Tier 3) high-quality large plots (\geq 6 ha; such as some from Labrière et al. (2018)).

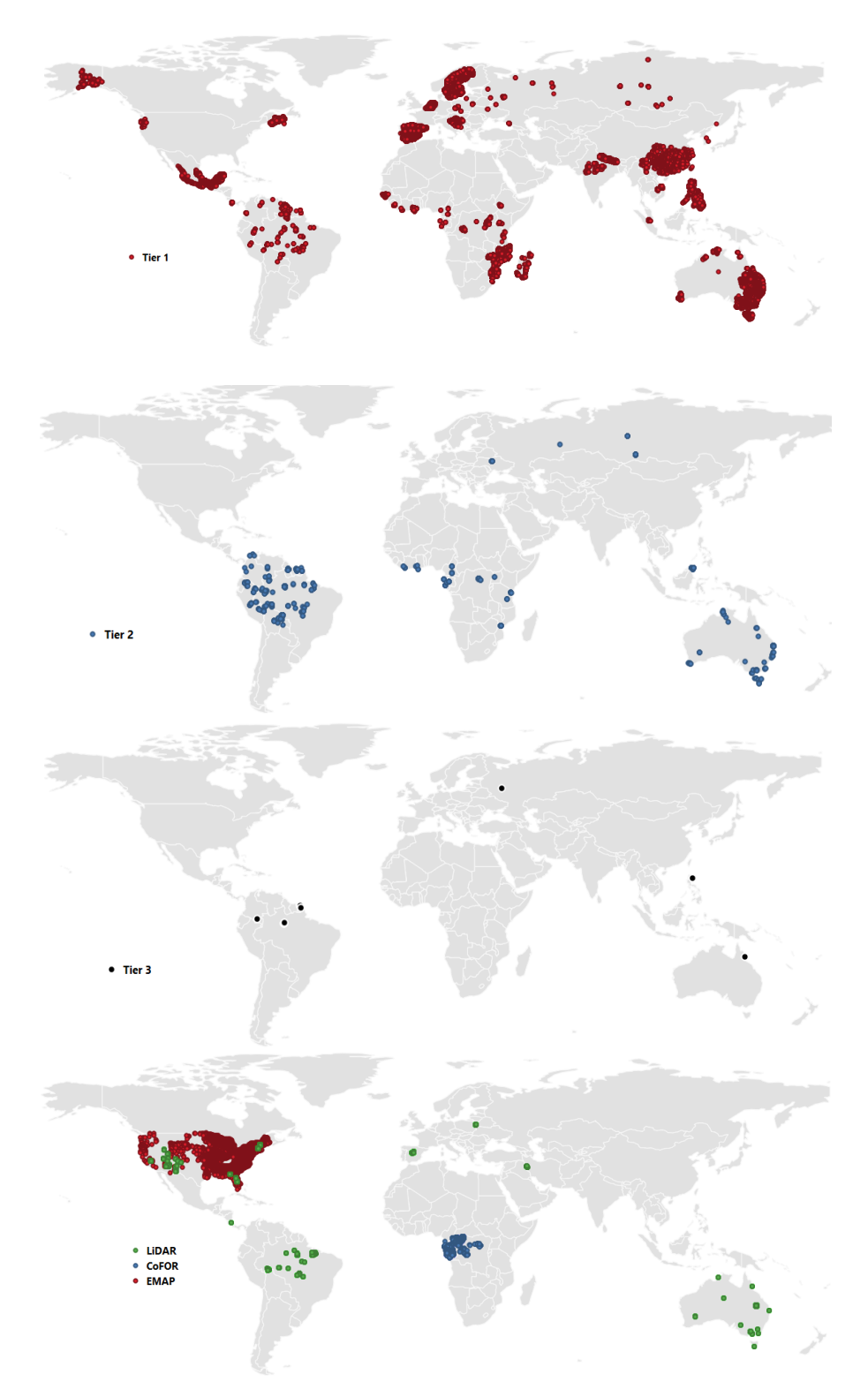
In addition to the above tiered classification, we use LiDAR-based AGB estimates at 100 m resolution from the Sustainable Landscape Brazil project (SLB), the National Ecological Observatory Network, USA (NEON) and the Terrestrial Ecosystem Research Network, Australia (TERN) processed by Labrière and Chave (2020a, b, c). Other region- or country-wise LiDAR transect collections are also included (over e.g., Kalimantan, the Brazilian Amazon and the Democratic Republic of Congo).

An independent data source concerns 1-km pixel forest management inventory data originating from the Congo basin Forests AGB (CoFor) dataset (Ploton et al., 2020). In this dataset, only pixels having at least five *in situ* forest management inventoried plots are proposed to be used. Similarly, the Environmental Monitoring and Assessment Program (EMAP) AGB also an aggregated data can be used. The dataset is an aggregate of 27-km hexagons estimated from the Forest Inventory and Analysis Program of the US Forest Service (Menlove and Healey, 2020).

These tiered plot data, the EMAP, LiDAR and the CoFor data are analysed separately in the descriptive plot-pixel comparisons (section 5.2). This categorization is favourable given the increasing recognition on use of LiDAR-based reference data.







	Ref	CCI Bio	omass Product Validation Plan v5	
esa	Issue	Page	Date	
	5.0	16	4-Dec-2024	



Figure 2. Geographical locations of plots and footprints of the reference datasets collected up to January 2024.

3.4. Data harmonization

For AGB product validation, the response design encompasses all steps leading to the assessment of differences between map and plot AGB (cf. Olofsson et al. 2014). The plots used in our comparison may have been surveyed at a different time than the map being assessed, they typically differ in spatial support (i.e., the area covered by individual plots) from the AGB map (AGB_{map}) pixels and they measure different spatial entities (average biomass over a pixel area versus forest biomass within a forest plot of known dimensions). Therefore, data harmonization is needed prior to the analysis of differences, as outlined below.

Differences between the inventory date of AGB plots and the reference year of the AGB map are harmonized using updated Intergovernmental Panel on Climate Change (IPCC) growth rates (IPCC 2019, Requena Suarez et al. 2019) following the approach described in Version 1 of the PVP (de Bruin et al. 2019a). For plots in tropical and subtropical ecological zones, age category dependent growth rates are available (IPCC 2019, Requena Suarez et al. 2019). In those cases, plot AGB values in the range 0-99 Mg/ha, 100-152 Mg/ha and above 153 Mg/ha are assumed to represent young secondary forest, old secondary forest (Van Breugel et al. 2007), and old growth stands (Brown et al. 1989, Clark and Clark 2000, Mello et al. 2016) respectively. Given the absence of data on plot forest age, mature forests with low biomass cannot be distinguished from young stands, which has potential implications for the proposed procedure. For temperate oceanic forests in Europe, boreal coniferous forests and tundra woodlands, no differentiation of growth rates as a function of age is used. The temporal adjustments by growth rates are applied up to a difference of ten years between the inventory date and the map reference year. Plots having a larger temporal difference are discarded in the analyses (see Section 3.1). The growth rate table in IPCC (2019) also reports different types of uncertainty estimates, such as confidence intervals (CI). The latter are translated into variances assuming a normal distribution.

Recall that the AGB plot data and the map have distinct sampling populations (see Section 3.2) in terms of both different spatial support and the inclusion of non-forested areas within map pixels. Harmonization of these differences is attempted by multiplying the temporally adjusted plot AGB by forest fraction. This forest fraction is computed by putting a 10% threshold on a tree cover product (Hansen et al. 2013) corresponding to the CCI Biomass map reference year. This is undertaken both at the pixel level and over larger aggregated blocks. In the rare case of more than one AGB plot occurring within a pixel, the average of the adjusted AGB per plot is used. The correction for forest fraction is applied only to plots with an area below 1 ha. Given that CCI dataset has multiple epochs, the 2010 tree cover was used to derive 2010 forest mask, 2000 tree cover data for the 2005 epoch but only after removing forest loss pixels from 2001 to 2005. For the 2015 and 2020 epochs, the tree cover 2010 dataset was used but without the forest loss pixels from 2011-2015 and 2011-2020, respectively.

The data harmonization procedure is pictured in Figure 3. The reference AGB obtained (either at pixel level or over aggregated pixel blocks) is referred to as AGB_{ref} .

	Ref	CCI Bio	CCI Biomass Product Validation Plan v5			
esa	Issue	Page	Date	biomass		
	5.0	17	4-Dec-2024	cci		

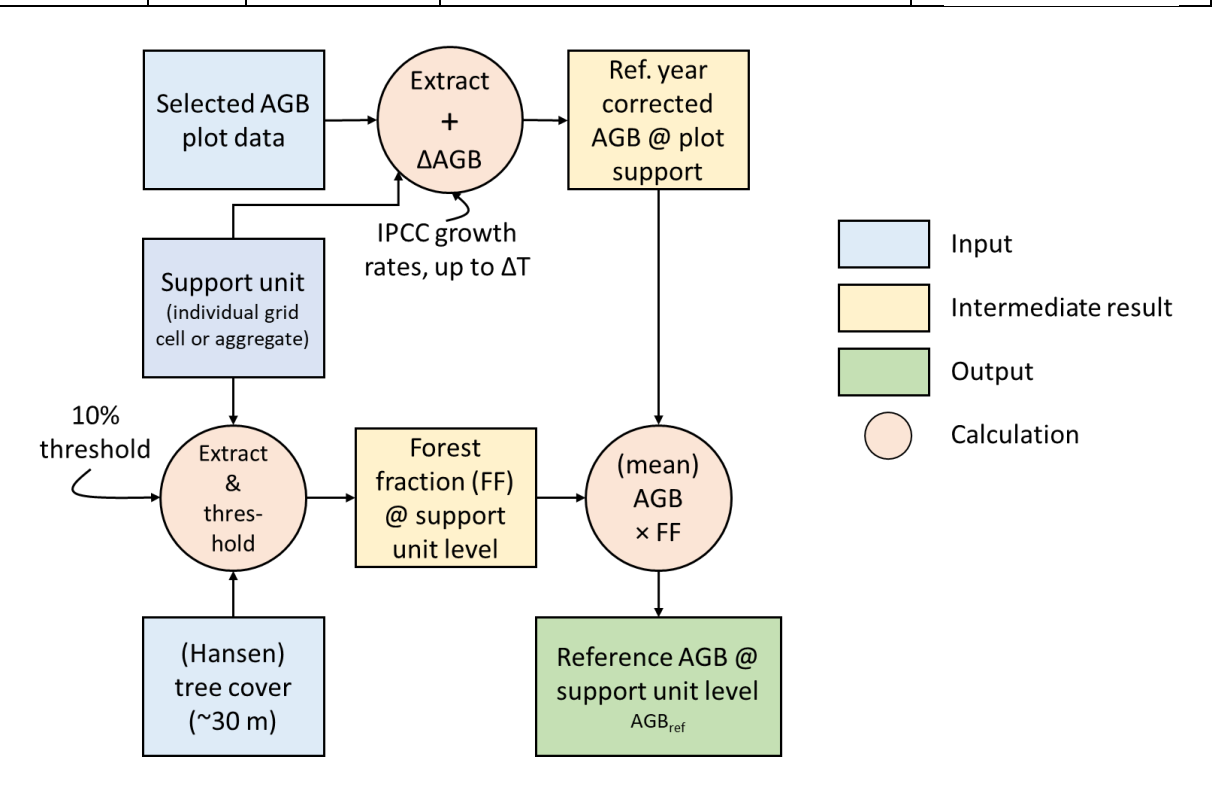


Figure 3. Overview of data harmonization steps.

	Ref	CCI Biomass Product Validation Plan v5	
esa	Issue	Page	Date
	5.0	18	4-Dec-2024



4. Database compilation for biomass changes

4.1. Sources of reference data

Reference data of changes in AGB (Δ AGB) in the past decade are required for the assessment of differences between the AGB maps derived from the CCI maps. While we already noted limited coverage in reference data for AGB stocks, the availability of AGB change (Δ AGB) reference measurements is even more limited. What we present here is a first attempt to collect and compile a dataset that could be useful for a comparison with Δ AGB estimates. The aim here is to explore availability and usefulness and compile the data for a first order comparison with AGB map-based change estimates. The current focus is on the period 2010-2020, as earlier data availability is more limited and, currently, no dedicated CCI Biomass AGB change products have been generated (only annual biomass maps).

The first set of reference data concerns re-measured NFI plot data acquired from Belgium, the Netherlands, Philippines and Sweden, where time 1 (T_1) and time 2 (T_2), that represent the times of measurement, are at least five years apart. For the NFIs, plot-level AGB has been estimated by the data providers but without uncertainty estimates. Also available are multi-date plot data for some of the plots from Tier 2 and Tier 3 described in the above section.

The second set of reference data comprises AGB maps derived locally in forests with re-measured plot inventories and two corresponding airborne LiDAR campaigns that took place between 2010 and 2019. These include maps from Brazil (Longo et al., 2016) and the USA (Johnson et al., 2010) where AGB mapping involved calibration of LiDAR height and plot AGB using power-law models. Also available are LiDAR-based maps from research projects in Bulgaria, Czech Republic, Ecuador, Spain, USA and Poland, derived using regression models that relate height and AGB. The LiDAR maps resampled to 100 m were used. Some of these maps have associated standard deviation (SD) layers (Appendix 2). Using LiDAR maps as reference allows skipping of the spatial harmonization step discussed in Section 3.4 and Figure 3.

The third set of reference data is country-level estimates of ΔAGB obtained from the Food and Agriculture Organisation (FAO) Forest Resources Assessment (FRA). These were derived by differencing the reported AGB Mg/ha from 2018 and 2010, where 2018 is computed as the average of 2015 and 2020 AGB Mg/ha estimates. The country's capability to conduct NFIs and derive FRA variables using remote sensing data was categorized on a scale of 1 to 5 (1=very poor; 5=very good).

4.2. Data processing and harmonization

The quality filtering criteria of \triangle AGB reference data are as follows:

- 1. Multi-date NFI plots can be filtered using tree cover loss datasets Hansen et al. (2013) to retain only plots without forest area changes after the latest measurement and before the 2020 map epoch. Plots more than 10 years apart from the map epoch can also be discarded;
- 2. LiDAR pixels can be discarded if there are AGB values in one epoch but not in another;
- 3. FRA data can be limited to countries with re-measured NFI or with "very good" NFI reporting capacity since 2010.

	Ref	CCI Bi	omass Product Validation Plan v5	
esa	Issue	Page	Date	
	5.0	19	4-Dec-2024	



Following this, the number of reference data retained after quality filtering compared to the original data was reported and mapped over eco-zones defined by Whittaker (1975). The coverage per eco-zone and country determined the suitability of reference data for global map assessments. For each reference dataset, histograms of the AGB distribution in two epochs are shown in Figure 5. The histograms of NFI and LiDAR selected data to derive the Δ AGB density and to assess the Δ AGB distribution at every aggregation level as described in Section 5.3.3 were also produced.

4.3. Characteristics of reference data

The characteristics of the compiled reference data are shown in Figure 4 (large plots not displayed yet, as the survey of relevant available data is still ongoing). The number of discarded data is largest for those associated with the FRA (90 %) since most countries do not have repeated NFIs. More than half (56 %) of the NFI plots were excluded either because they were outdated, or the sites had been deforested after the second measurement and before 2020. Almost no LiDAR pixels (<1%) were filtered out as reference since the repeated LiDAR surveys all took place in the past decade and almost all pixels were associated with data collected during the 2010-2021 period. The reference data were mostly found in the temperate and tropics, but these are still under-represented, as were all other eco-zones. The selected FRA data, though small in size, are relevant to all ecozones. Despite its smaller size, the NFI dataset had broader eco-zone coverage than the LiDAR dataset. That was because NFIs are surveyed over entire countries while LiDAR campaigns are typically confined to certain forested zones or regions. The current reference data do not include NFIs and LiDAR data from Africa, Australia or Brazil (where some transects and sites from the SLB project were flown over again during the EBA project; see Tejada et al. 2019 for details). The ΔAGB distributions of LiDAR and NFI data at different aggregation levels (Section 5.4) are shown in Figure 5. The highest density of data is observed for small AAGB but there are also several reference data indicating large AGB gains and losses.

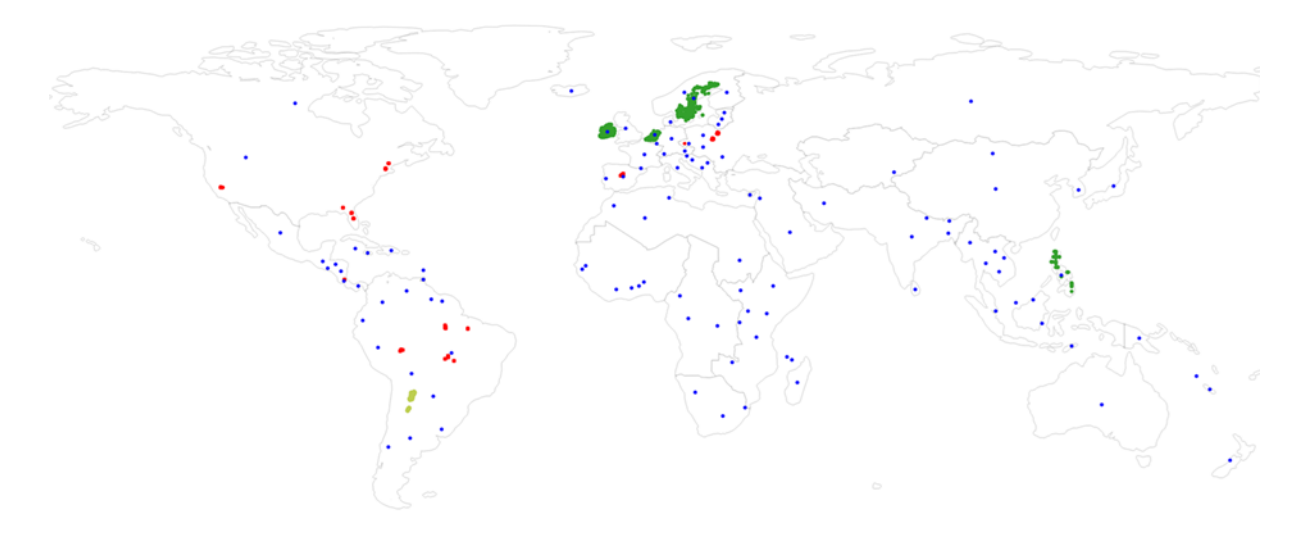


Figure 4. Coverage of the reference data per major ecological zone (a) and the map of the selected reference data (b). The reference data are already quality-filtered.

	Ref	CCI Bio	omass Product Validation Plan v5	
esa	Issue	Page	Date	biomass
Allen.	5.0	20	4-Dec-2024	cci

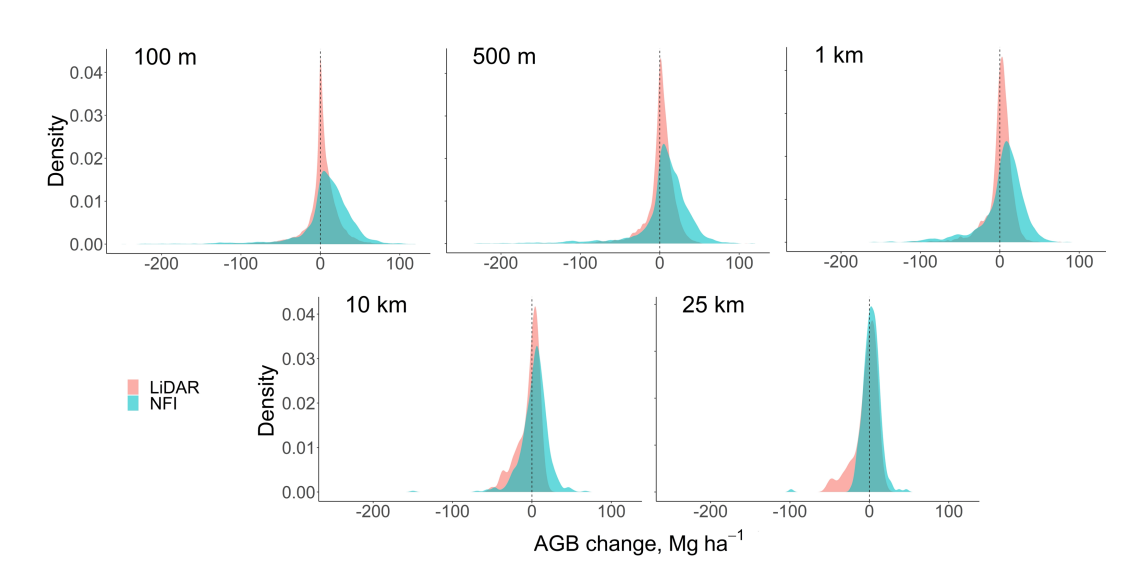


Figure 5. Distributions according to NFI and LiDAR data for the five aggregation levels.

esa	Ref	CCI Biomass Product Validation Plan v5	
	Issue	Page	Date
	5.0	21	4-Dec-2024



5. Map-plot comparisons

5.1. Assumptions

After adjustments for temporal discrepancies and partial forest fraction and having at least ten *in situ* sites within a reference biomass range, we assumed mean AGB_{ref} computed from the reference data in Tiers 1 and 2 to be unbiased. For Tier 3 data we relaxed the requirement of 10 plots per biomass range because these data were recorded over large footprints (≥ 6 ha) and the measurements followed a strict protocol.

When reporting mean differences (i.e., AGB_{map} - AGB_{ref}) and root mean squared difference (RMSD) over different spatial strata, we assumed that comparisons of map data and *in situ* data within these were representative of those strata. For the descriptive analyses (Section 5.2), we further assumed that mapplot comparisons are mutually independent but in the proposed geostatistical approaches (Chapter 6), this assumption was relaxed.

5.2. Descriptive analyses

For tabulation, 50 Mg/ha wide AGB_{ref} bins were used up to 400 Mg/ha, while AGB_{ref} values above 400 Mg/ha were grouped in a single bin (i.e., 0-50, 50-100 ... 350-400 and > 300 Mg/ha). For each bin, the tables list at least the mean AGB_{ref} , mean AGB_{map} , mean AGB_{map} - AGB_{ref} (MD), and the RMSD between AGB_{ref} and AGB_{map} .

For plotting, 25 Mg/ha wide bins were used up to 350 Mg/ha along with a single bin for all higher AGB_{ref} values. The plots have AGB_{ref} on the x-axis and AGB_{map} on the y-axis. Mean (AGB_{ref}, AGB_{map}) pairs are shown using a point symbol while the interquartile ranges of AGB_{map} per bin are depicted by whiskers. An example is shown in Figure 6.

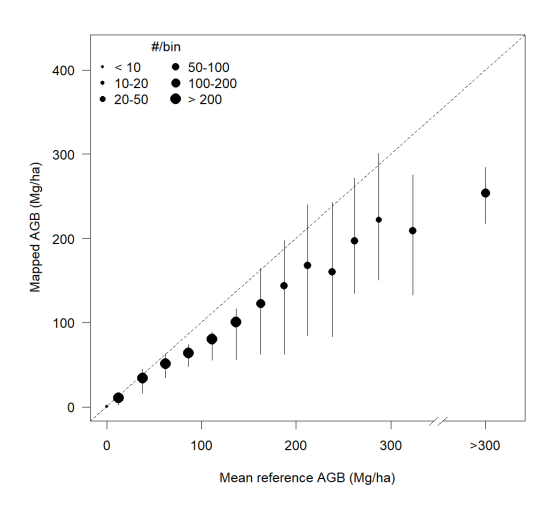
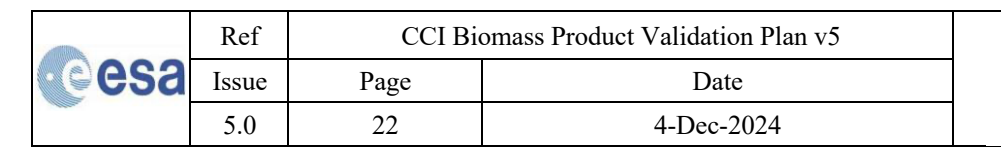


Figure 6. Example of a AGB_{map} - AGB_{ref} comparison plot taken for epoch 2020 from the PVIR 5.0 report (last accessed July, 2024).

A straightforward way of analysing AGB_{map} - AGB_{ref} differences was anticipated in Section 3.3. To account for the expected differences in the accuracy of plots in different size categories, plots in different tiers





can be analysed separately. Under the above unbiasedness assumption (Section 5.1), mean differences between harmonized *in situ* data and map values aggregated over bins covering ranges of reference AGB values were interpreted as map bias, per tier. However, note that binning of *in situ* data that are affected by random errors may falsely suggest map bias. This has been demonstrated for the within-pixel sampling error in the latest Product Validation and Intercomparison Report (PVIR) (de Bruin et al., 2020b, Figures 17 and 18). To empirically verify the assumption of unbiased *in situ* data, the analyses were conducted for each of the tier's other data sources and the consistency of results was assessed whenever data volume allowed.

An alternative to the tiered approach is to weight AGB_{map} - AGB_{ref} differences within bins using inverse variance weighting based on the sum of the *in situ* measurement error variance, the variance of the error introduced at the data harmonization steps, and the plot-pixel sampling error. These error variances are explained in Section 6.1. Such an approach is only possible if sufficient data are available for assessing spatial correlation structures of the latter error component for the smallest footprint size. When weighted (AGB_{ref} , AGB_{map}) pairs are computed, weighted quantiles and RMSD were used for tabulation and plotting.

5.3. Stratification and spatial aggregation for stocks

5.3.1. Comparisons at 0.1° cell resolution

Depending on how data are used, biomass map users such as climate modellers and REDD+ communities may be interested in uncertainties over larger support units, such as square pixel blocks. This preference was shared by climate modellers themselves in a survey conducted in 2018 (Quegan and Ciais 2018). Aggregation of biomass predictions and measurements over larger spatial units often results in a partial cancelling out of *random* prediction errors and measurement errors. Note that this does not hold for systematic error or bias. Therefore, aggregation is expected to improve the precision of map and harmonized plot data if both map and multi-plot data are averaged over larger spatial units.

To assess the CCI Biomass map at a resolution commonly used by climate modellers, AGB_{map} - AGB_{ref} comparisons were also made over multi-pixel blocks at 0.1° cell resolution. In this case, correction for partial forest fraction (see above) was undertaken at the level of the coarse resolution cells. Mean AGB_{ref} at 0.1° cell resolution was computed by multiplying forest fraction at the 0.1° cell level with the mean temporally adjusted AGB plots in that cell (see Figure 3).

Three options were considered for calculating the latter mean temporally adjusted AGB at the 0.1° cell level.

- Using unweighted means for each of the tiers and other data sources (LiDAR/CoFoR) separately (see Section 5.2).
- Inverse variance weighting of *in situ* data based on the sum of the AGB measurement error variance, the variance of the error introduced at the data harmonization steps (Section 3.4), and the within-pixel sampling error. This option still assumes mutual independence of plot data but explicitly accounts for differences in the quality of plot data.
- Relaxing the mutual independence of *in situ* data. Another option is to compute block averages through a block kriging approach (Goovaerts 1999, Malone et al. 2013).

Our aim is to compare the above options but the latter two are only feasible if sufficient data are available for assessing spatial correlation structures (variograms $\gamma_{AGB}(h)$) of AGB for the smallest plot

	Ref	CCI Biomass Product Validation Plan v5		
esa	Issue	Page	Date	
	5.0	23	4-Dec-2024	



size used in the analyses. The resulting AGB reference values were then compared with the average AGB_{map} over the corresponding 0.1° cells.

5.3.2. Comparisons at native map resolution

Other map users may be interested with the validation of maps at native resolution. In such a case, the biomass estimates between reference data can be compared with pixel-level biomass. The comparisons can be per based on different tiers according to plot sizes and even reference data type e.g., LiDAR only for map-map comparisons (see PVIR 5.0).

5.3.3. Ecoregions

 AGB_{map} – AGB_{ref} comparisons at 0.1° cell resolution (see above) were also stratified at biome scales according to the map of Dinerstein et al. (2017; see https://ecoregions2017.appspot.com/). The biomes include Once downloaded, the original vector maps were rasterized to 0.1° resolution and the raster cells were assigned to the category covering the largest portion of the cell area.

5.4. Spatial aggregation for AGB change

Similarly to assessing AGB stocks, grid cells for \triangle AGB assessments were used if they met the minimum number of reference data requirements (Araza et al., 2022). Hence grid cells with very few reference data were excluded from the analysis. Selected data inside grid cells were assumed to capture the composition of forest structure at the selected grid cell resolution. The AGB averages per epoch from NFI plots and LiDAR pixels at grid cells were estimated as weighted means where reference data with high uncertainty received smaller weights in the averaging. The weights were inversely proportional to the variance of an NFI plot or a LiDAR pixel (Araza et al., 2022). The AGB averages of all grid cells were harmonized, particularly those that included non-forest areas to minimize the discrepancy in forest areas between the reference data and maps (i.e., map pixels include both forest and non-forest). This spatial aggregation was proposed to be undertaken iteratively at different aggregation levels in the context of different map users requiring products from fine to coarse resolutions (Table 2).

Table 2. Details of the ΔAGB map-reference data comparisons and the selection of grid cells.

Assessment spatial scale	NFI grid cell selection criteria	LiDAR grid cell selection criteria
100×100 m ² (100 m)	all	All
500×500 m ² (500 m)	all	All
$1\times1 \text{ km}^2 (1 \text{ km})$	>1 plots	All
$10 \times 10 \text{ km}^2 (10 \text{ km})$	>4 plots	>14 pixels
25×25 km ² (25 km)	>9 plots	>19 pixels

	Ref	CCI Bio	omass Product Validation Plan v5
esa	Issue	Page	Date
	5.0	24	4-Dec-2024



6. Spatial uncertainty modelling for biomass

6.1. Definition of the error model

Even though the *in situ* AGB data were assumed unbiased, they are not error-free and therefore comparisons between AGB maps and AGB *in situ* data should be accompanied by an uncertainty analysis. The first step in such analysis is the definition of the error model. We propose an additive model expressing the difference between a map prediction AGB_{map} and reference AGB_{ref} at pixel x (denoted as D(x)) as a random variable composed of five zero mean random error components and a map bias component (Equation 1):

$$D(x) = M(x) - (Plt(x) + Pos(x) + H(x)) + S(x) + b(x)$$
(1)

where M(x) the map biomass error at location x, Plt(x) is the plot measurement error (Réjou-Méchain et al. 2017), Pos(x) is a positional error component, H(x) is the error introduced at the data harmonization steps (Section 3.4), S(x) is a within-pixel sampling error component, and b(x)) is the map bias (i.e., the difference $AGB_{map}(x) - AGB^*(x)$, where the latter term is the true biomass density for pixel x. The within-pixel sampling error, S(x), arises because the AGB plot size is usually small compared to the ~ 1 ha AGB map pixel (see Appendix 1). It is defined as $AGB^*(x) - AGB^*_{plot}(x)$, where the latter term is the true biomass at the spatial support of in situ data within the pixel. A pixel footprint covered by a homogeneous forest biomass population has sub-pixel biomass variation, and the plot samples only part of that. Pixel footprints partly covered with forest undergo a harmonization procedure as explained in Section 3.4. Note that S(x), Plt(x), Pos(x), S(x) and H(x) are random variables whose values are unknown but can be described by probability distributions (Heuvelink, 2005).

All random error terms at the right-hand side of Equation (1) (i.e., all terms except b(x)) are assumed to be zero mean and mutually uncorrelated. If the plot is small relative to the pixel size, Pos(x) is not relevant unless the plot is at the edge of the pixel; all that matters is that it is located within the pixel. Earlier analyses using a conservative distance decay function for sampling map-plot residuals revealed that indeed Pos(x) is small compared to the other error components. Omitting Pos(x), the variance of the difference between a map prediction AGB_{map} and reference AGB_{ref} at pixel x equals the sum of the remaining error variances (Equation 2):

$$Var(D(x)) = Var(M(x)) + Var(Plt(x)) + Var(S(x)) + Var(H(x))$$
 (2)

In our geostatistical modelling, we consider the spatial correlation of M(x), because errors in the AGB maps can be spatially correlated and we need to account for this in our model-based inference. We take into account this spatial correlation for purposes of assessing the joint AGB uncertainty when aggregating map data to larger support units, such as pixel blocks, countries or other regions of interest. The spatial correlation of M(x) is modelled using (biome-specific) variograms, $\gamma_M(h)$, where h refers to a distance lag.

We aim to model the bias b(x) as a function of AGB_{map} and other spatially exhaustive covariates, as described in Section 6.3.1.

esa	Ref	CCI Bio	omass Product Validation Plan v5	
	Issue	Page	Date	
	5.0	25	4-Dec-2024	l



6.2. Identification of the error model

6.2.1. Overview

Table 2 provides an overview of the approaches for estimating the parameters of the uncertainty model described above. First results confirm an inverse relationship between Var(Plt(x)) and plot size, while b(x) is often positive when the predicted AGB value is small (i.e., low AGB_{map} values tend to exceed AGB_{ref}) and negative when they are large (i.e., high AGB_{map} values in the map tend to be less than AGB_{ref}).

Table 3. Estimation methods for the parameters of the uncertainty model.

Component	Estimation approach
b(x)	Modelled as a function of AGB_{map} and spatially exhaustive covariates such as biome (Dinerstein et al. 2017), topographic variables and proxies for anthropogenic activity, using a random forest model (Breiman 2001) trained on observed differences, d_i , between AGB_{map} and AGB_{ref} data.
Var(M(x))	Square of the SD of the (zero mean) prediction error accompanying the CCI Biomass maps, as described in Quegan et al., (2017) and Santoro and Cartus (2019).
Var(Plt(x))	For a subset of plots having individual tree measurements, (Réjou-Méchain et al. 2017) biomass R-package is used. For other plots lacking such data, $Var(Plt(x))$ is predicted by a random forest model trained on the subset having individual tree measurements, using AGB _{map} , plot size and biomes as explanatory variables.
Var(S(x))	$Var(AGB_{pixel} - AGB_{plot}) = Var(AGB_{pixel}) + Var(AGB_{plot}) + 2 \cdot \sigma_{AGB_{pixel}, AGB_{plot}}$, where $\sigma_{AGB_{pixel}, AGB_{plot}}$ is the covariance of AGB_{pixel} and AGB_{plot} . All terms on the right-hand side of this equation are obtained from variograms of small, contiguously clustered sites within relevant Biomes, using change of support geostatistics (Goovaerts 1999, Malone et al. 2013). If nearby sites have different inventory dates, temporal adjustment to a common date is required, as described in Section 3.4.
Var(H(x))	Variance of mathematical operations applied to random variables in the harmonization steps.
$\gamma_{AGB}(h)$	Variogram model fitted to experimental semivariances of AGB with a spatial support of the smallest plot size used. Used data are small-plot AGB _{plot} data, LiDAR -derived AGB or AGB _{plot} from larger plots, followed by deconvolution using a nugget-to-sill ratio borrowed from LiDAR data. Following Christensen (2011), the mean of $Var(Plt(x))$ is subtracted from the nugget.
$\gamma_M(h)$	Variogram model fitted to experimental semivariances of residuals between AGB _{map} and AGB _{ref} after subtracting the bias $b(x)$. This variogram has a spatial support of map pixels. To correct for the other error sources, the mean variances $Var(Plt(x)), Var(S(x))$ and $Var(H(x))$ are subtracted from the nugget, following Christensen (2011). Scaling of the residuals may be needed to transform $M(x)$ to homoscedasticity (see Section 6.2.3).

6.2.2. Variograms of AGB from small plots

As shown in Table 3, prediction of Var(S(x)) requires variograms of AGB from small, contiguously clustered sites located within relevant biomes $(\gamma_M(h))$. At the stage of writing, we only have access to a limited number of data coming from research plots, clustered NFI plots, and LiDAR-derived AGB data

esa	Ref	CCI Bi	omass Product Validation Plan v5
	Issue	Page	Date
	5.0	26	4-Dec-2024



from small footprints acquired over two forest sites in Remningstorp, Sweden, and Lope, Gabon (i.e., a boreal and a tropical forest site, respectively). The former ALS datasets were acquired in the framework of the airborne ESA BIOSAR (Ulander et al., 2011).

Subplots from research plots are often larger (0.25ha) than the smallest plots of our dataset (a few plots are only 0.01ha). Variograms at the smallest support size will be obtained by variogram deconvolution (Goovaerts 2008) with a fixed nugget-to-sill ratio obtained from fine resolution AGB data, such as LiDAR-derived AGB. Following Christensen (2011), the mean variance of the plot measurement error is subtracted from the nugget variance.

6.2.3. Variograms of map error at the spatial support of map pixels

Spatial aggregation of uncertainty over larger support units (see section 6.3.4) requires variograms of $M(\cdot)$ at pixel support $(\gamma_M(h))$. The uncertainty layer of the CCI Biomass maps and the other uncertainties considered in Section 6.1 acknowledge that we expect Var(D(x)) to vary over space (i.e., it is heteroscedastic). In other words, we recognize that at some locations, larger deviations between AGB_{map} and AGB_{ref} are more likely to occur than at other locations. Again, the (Christensen 2011) approach for heterogeneous measurement error variances will be used for estimating the variogram of the unobserved $M(\cdot)$ at pixel support, using estimated values for each error component as listed in Table 3. If necessary, observed realizations of D(x) - b(x) are scaled by $\sqrt{Var(M(x))}$ aiming to achieve homoscedasticity.

6.3. Model-based prediction

6.3.1. Bias trend prediction

Different forest types, climatic gradients, topography and AGB itself have been found to affect bias in AGB predictions (Chave et al. 2004, Rodríguez-Veiga et al. 2019, Santoro et al. 2015). We try to model this bias as a function of AGB_{map} and its textural properties as well as other spatially exhaustive covariates such as biome (Dinerstein et al. 2017), topographic variables (elevation, slope), canopy height and a proxy for anthropogenic activity (population density) using a random forest model (Breiman 2001). The approach is documented in more detail in Araza et al. (2022).

The predictive power of the covariates is evaluated using variable importance measures while sensitivity of the modelled trends to the inputs is assessed using partial dependence plots (Greenwell 2017). If fitting the bias trend model is successful, the random forest model is used in predictive mode to predict a global bias layer b(x). The statistical significance of predicted bias is assessed using the prediction standard errors obtained with Wager's et al. (2014) infinitesimal jack-knife approach.

6.3.2. Error budgeting

The error model presented in Section 6.1 allows comparison of Var(D(x)) observed over AGB_{ref} bins with the sum of the error variances at the right-hand side of Equation (2). In de Bruin et al. (2019b, 2020b), a similar partial comparison was used to assess whether the error layer provided with the CCI

esa	Ref	CCI Bio	omass Product Validation Plan v5	
	Issue	Page	Date	
	5.0	27	4-Dec-2024	



Biomass map is consistent with considered error variances. This comparison can only be completed if the error model has been fully identified (Section 6.2).

6.3.3. Block kriging for map-plot comparison at supra pixel support

Section 5.3.1 referred to a third option for computing the mean temporally adjusted AGB_{ref} at the spatial support of 0.1° cells by block kriging. This is achieved by computing block averages of AGB from within-block and nearby temporally adjusted plot AGB using the small plot variograms introduced in Section 6.2.2 and block kriging that accounts for different error variances of the plot data (Malone et al. 2013). The procedure also computes the variance of the prediction error. Correcting for forest fraction (section 3.4), AGB_{ref} at 0.1° cell level is obtained, which is compared with the average AGB_{map} over the 0.1° cell. It is repeated here that this procedure is only possible if variograms of AGB at the spatial support of the smallest plots are available for the different forest types.

6.3.4. Spatial aggregation of random error

Spatially uncorrelated zero-mean errors tend to cancel out when aggregating over larger spatial units, but this effect is less pronounced when errors are spatially correlated. We model the latter effect using the variograms introduced in section 6.2.3. From the variograms and the distance matrix for all pixel pairs, x_i , x_j contained in a support unit, a covariance matrix, Σ , is computed with elements $\sigma_{i,j}$. The variance of the map error over the support unit is then predicted by summing the elements of Σ and division by n^2 (Equation 3):

$$Var(aggr) = \frac{1}{n^2} \sum_{i=1}^{n} \sum_{j=1}^{n} \sigma_{i,j}$$
(3)

esa	Ref	CCI Bio	omass Product Validation Plan v5
	Issue	Page	Date
	5.0	28	4-Dec-2024



7. Map inter-comparison

7.1. Stability of $AGB_{map} - AGB_{ref}$ among CCI Biomass products

According to the World Meteorological Organization (2011), stability is the extent to which the error of a product remains constant over time. To exploratively assess the local stability of the plot-map differences (d_i) over the multiple AGB epochs (i.e., 2010 and 2017 - 2020) produced within the CCI Biomass project, we suggest to produce scatterplots of d_i for each combination of map reference years, as exemplified in Figure 7.

The map producer may want to know where the largest instabilities in the residuals occur. Such information can be provided by plotting the locations of chosen tails of the distribution of differences in d_i for different combinations of reference years (e.g., the 5% of sites with the most negative differences and the sites of the 5% largest positive differences). Alternatively, sites where the instability exceeds a particular threshold (e.g., 10%, as proposed by the World Meteorological Organization²) can be of interest.

² https://gcos.wmo.int/en/essential-climate-variables/biomass/ecv-requirements

	esa	Ref	CCI Bi	omass Product Validation Plan v5	
		Issue	Page	Date	Ó
		5.0	29	4-Dec-2024	



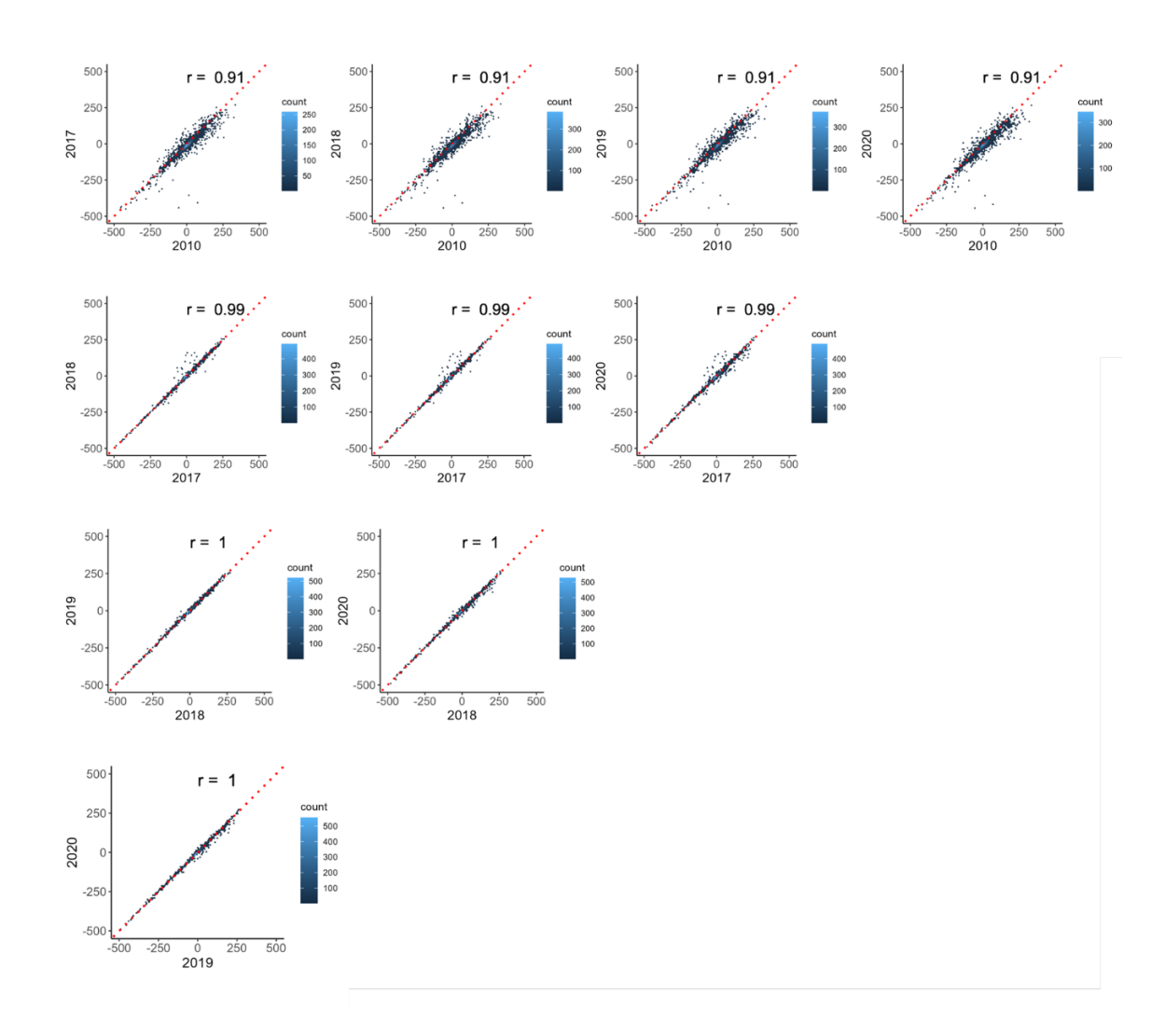


Figure 7. Example of AGB residuals between harmonized Tier 1–3 plot data and mapped AGB at 0.1° cell level for each combination of map reference years. The red dashed line is the 1:1 line.

7.2. Comparison of CCI Biomass maps with other AGB products

This task consists of the comparison of the CCI Biomass maps with other AGB products covering a given geographic extent, as well as comparison of map bias based on AGB reference data. The comparison aims to complement the product validation with the following information: evaluation of consistency between different products; identification of areas with larger disagreements and assessment of whether these areas need further study; assessment of strengths and weaknesses of different datasets

esa	Ref	CCI Bi	omass Product Validation Plan v5	
	Issue	Page	Date	
	5.0	30	4-Dec-2024	



based on the analysis of the data and methods used to produce the maps; and increased awareness and acceptance of CCI Biomass products within the international community.

The map inter-comparison involves the following steps. Firstly, datasets to be compared (i.e., regional or global maps) are identified and acquired. Secondly, the datasets are harmonized with CCI Biomass maps in terms of spatial and temporal support (see section 3.4) as well as thematic content (e.g., biomass unit). Thirdly, the following comparison metrics are computed at pixel level and at aggregated grid resolution (e.g., 0.1°):

- 1. Comparison statistics, global and across continents and biomes
 - Mean (absolute) difference
 - Histogram of differences
 - Root Mean Square Difference
 - Linear correlation
- 2. Comparison maps:
 - Difference maps
 - Relative difference maps, using the CCI Biomass maps as reference
- 3. Comparison plots of mapped data:
 - Scatterplots or whisker plots such as exemplified in Figure 8.
 - Histograms and cumulative distributions
- 4. Comparison plots of mapped data against harmonized AGB plot data, such as exemplified in Figure 8.

The map comparison could be expanded to biomass change datasets using a similar framework.

esa	Ref	CCI Bio	omass Product Validation Plan v5
	Issue	Page	Date
	5.0	31	4-Dec-2024



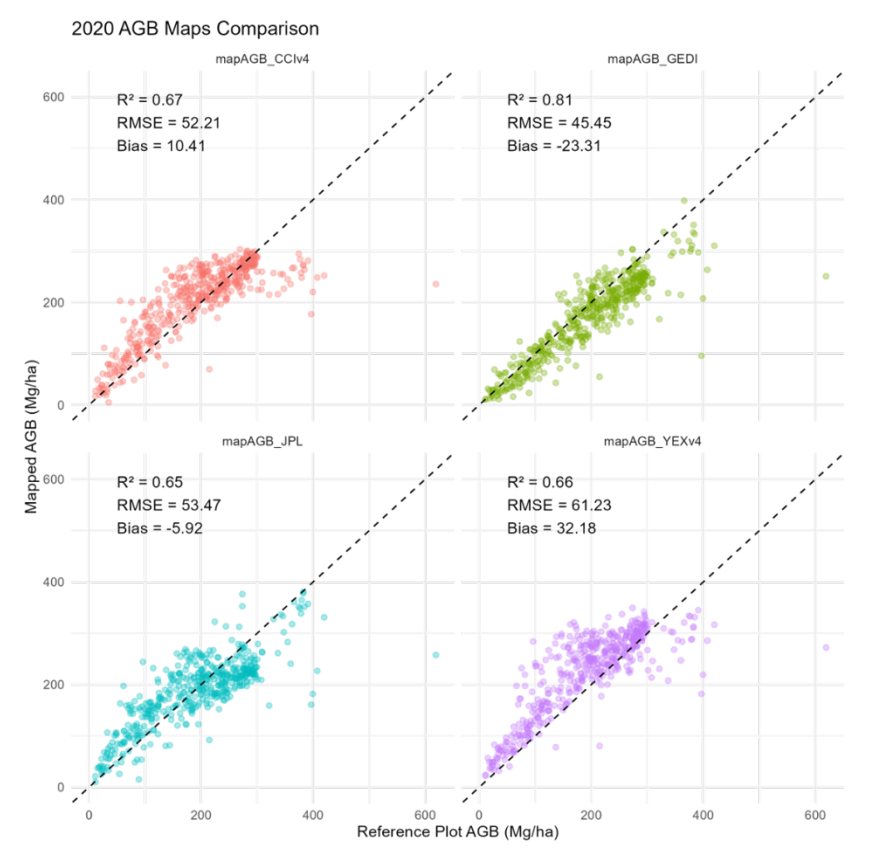
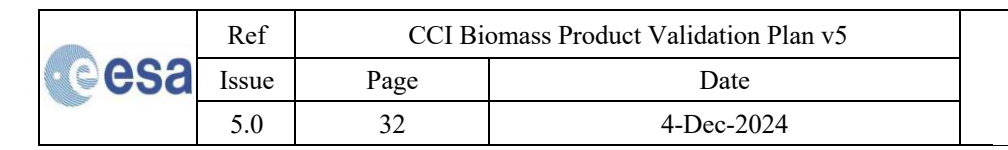


Figure 8. Comparison of different global biomass maps against harmonized plot data for the whole of Brazil. The CCI map is version 4 and the YEXv4 biomass map is from a previous version of Fendrich et al. (under review as of Febr, 2025). The value of bias refers to the mean AGB of the full dataset.





8. Expert assessment

The Expert Assessment is an essential quality control and feedback mechanism, aimed at assessing the users' acceptance of CCI Biomass products, evaluating their quality and limitations from the users' perspective, and obtaining recommendations for improvements. The output of the Expert Assessment consists of an Expert Survey report.

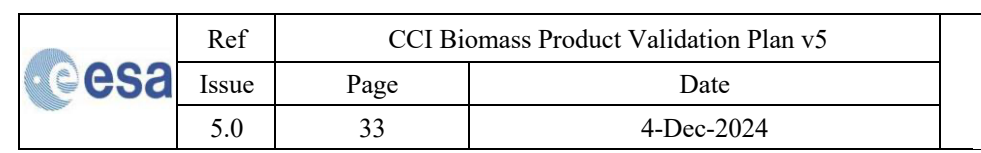
The Expert Assessment is performed using standard questionnaires, which are produced for each CCI Biomass product. The questionnaires aim to assess:

- User satisfaction.
- Product usability.
- Delivery system (timing, delivery method, naming, format, etc.).
- Product quality and limitations related to spatial and temporal resolution.
- Applicability of the products for climate modelling.
- Need of capacity building (optional).
- Future data and product requirements.

To support users in assessing the CCI Biomass products using their own data, an R-workflow is being implemented in tools intended for distinct user groups: This consists of:

- (1) An online interactive tool for occasional users, which provides easy access to the analysis methods described in this validation plan.
- (2) An offline toolbox for technical users who want to integrate the analysis methods in their own workflow (i.e., third parties who conduct independent validation). Error! Reference source not found. shows a screenshot of a prototype of the online interactive tool; the local version can be found at: GitHub arnanaraza/Plot2Map: Plot-to-map comparison of aboveground biomass workflow. The local version has been tested by users from the University of Leicester, Forest Research in the UK and the World Resources Institute. The main functionalities of the R workflow include pre-processing of different forest inventory configurations (e.g., plot shapes), estimation of measurement error for plot data with and without tree-level measurement and visualization of plot-to-map comparisons.

The tool *Plot2Map* can also be accessed using the Multi-mission Algorithm Platform (MAAP) (Albinet et al., 2019). Through the MAAP, global map users can use their own (country) data to validate global maps while retaining the privacy of their reference data such as NFIs. See Figure 9 for sample MAAP implementations. The user manual on how to use Plot2Map in the MAAP using the ESA account can be found here: Plot2Map MAAP User Guide - Google Docs





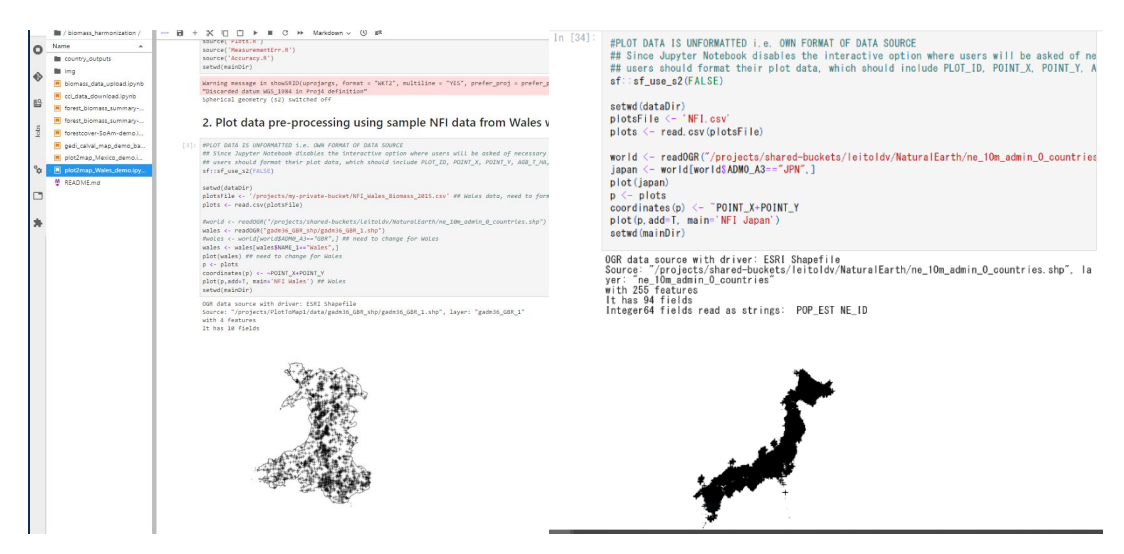


Figure 9. Wales (left) and Japan (right) country cases of validating the CCI map through the MAAP.

esa	Ref	CCI Bio	omass Product Validation Plan v5
	Issue	Page	Date
	5.0	34	4-Dec-2024



References

- Albinet, C., Whitehurst, A. S., Jewell, L. A., Bugbee, K., Laur, H., Murphy, K. J., ... & Duncanson, L. (2019). A joint ESA-NASA multi-mission algorithm and analysis platform (MAAP) for biomass, NISAR, and GEDI. *Surveys in Geophysics*, 40(4), 1017-1027.
- Armston, J., Tang, H., Hancock, S., Marselis, S., Duncanson, L., KELLNER, J., ... & Dubayah, R. O. (2020). AfriSAR: Gridded Forest Biomass and Canopy Metrics Derived from LVIS, Gabon, 2016. *ORNL DAAC*.
- Araza, A., De Bruin, S., Herold, M., Quegan, S., Labriere, N., Rodriguez-Veiga, P., ... & Lucas, R. (2022). A comprehensive framework for assessing the accuracy and uncertainty of global above-ground biomass maps. *Remote Sensing of Environment*, 272, 112917.
- Avitabile, V., Balzter, H., de Bruin, S., Carreiras, J., Carvalhais, N., Quegan, S., Tansey, K. and Rodriguez-Veiga, P. (2015) DUE GlobBiomass Validation Protocol, Wageningen University and Research Centre.
- Breiman, L. (2001) Random Forests. Machine Learning 45(1), 5-32.
- Chave, J., Condit, R., Aguilar, S., Hernandez, A., Lao, S. and Perez, R. (2004) Error propagation and scaling for tropical forest biomass estimates. Philosophical transactions of the Royal Society of London. Series B, Biological sciences 359(1443), 409-420.
- Christensen, W.F. (2011) Filtered Kriging for Spatial Data with Heterogeneous Measurement Error Variances. Biometrics 67(3), 947-957.
- de Bruin, S., Herold, M. and Araza, A. (2019a) CCI Biomass Product Validation Plan, Year 1, Version 1.
- de Bruin, S., Herold, M., Araza, A., Kay, H. and Lucas, R. (2019b) Product validation & intercomparison report, year 1, version 1.1.
- de Bruin, S., Herold, M. and Araza, A. (2020a) CCI Biomass Product Validation Plan, Year 2, Version 2.
- de Bruin, S., Herold, M., Araza, A., Kay, H. and Lucas, R. (2020b) Product validation & intercomparison report, year 2, version 2.
- Dinerstein, E., Olson, D., Joshi, A., Vynne, C., Burgess, N.D., Wikramanayake, E., Hahn, N., Palminteri, S., Hedao, P., Noss, R., Hansen, M., Locke, H., Ellis, E.C., Jones, B., Barber, C.V., Hayes, R., Kormos, C., Martin, V., Crist, E., Sechrest, W., Price, L., Baillie, J.E.M., Weeden, D., Suckling, K., Davis, C., Sizer, N., Moore, R., Thau, D., Birch, T., Potapov, P., Turubanova, S., Tyukavina, A., de Souza, N., Pintea, L., Brito, J.C., Llewellyn, O.A., Miller, A.G., Patzelt, A., Ghazanfar, S.A., Timberlake, J., Klöser, H., Shennan-Farpón, Y., Kindt, R., Lillesø, J.-P.B., van Breugel, P., Graudal, L., Voge, M., Al-Shammari, K.F. and Saleem, M. (2017) An Ecoregion-Based Approach to Protecting Half the Terrestrial Realm. BioScience 67(6), 534-545.
- Goovaerts, P. (1999) Geostatistical Tools for Deriving Block-Averaged Values of Environmental Attributes. Geographic Information Sciences 5(2), 88-96.
- Goovaerts, P. (2008) Kriging and Semivariogram Deconvolution in the Presence of Irregular Geographical Units. Mathematical Geosciences 40(1), 101-128.
- Greenwell, B.M. (2017) pdp: An R package for constructing partial dependence plots. R Journal 9(1), 421-436.
- Hansen, M.C., Potapov, P.V., Moore, R., Hancher, M., Turubanova, S.A., Tyukavina, A., Thau, D., Stehman, S.V., Goetz, S.J., Loveland, T.R., Kommareddy, A., Egorov, A., Chini, L., Justice, C.O. and Townshend, J.R.G. (2013) High-Resolution Global Maps of 21st-Century Forest Cover Change. Science 342(6160), 850-853.
- Hijmans, R.J. (2017) raster: Geographic Data Analysis and Modeling.
- Horn, B. (1981) Hill shading and the reflectance map. Proceedings of the IEEE 69, 14-47.
- Johnson, B. R., Kuester, M. A., Kampe, T. U., & Keller, M. (2010, July). National ecological observatory network (NEON) airborne remote measurements of vegetation canopy biochemistry and structure. In 2010 IEEE International Geoscience and Remote Sensing Symposium (pp. 2079-2082). IEEE.
- Labrière, N., Tao, S., Chave, J., Scipal, K., Toan, T.L., Abernethy, K., Alonso, A., Barbier, N., Bissiengou, P., Casal, T., Davies, S.J., Ferraz, A., Hérault, B., Jaouen, G., Jeffery, K.J., Kenfack, D., Korte, L., Lewis, S.L., Malhi, Y., Memiaghe, H.R., Poulsen, J.R., Réjou-Méchain, M., Villard, L., Vincent, G., White, L.J.T. and Saatchi, S. (2018) In SituReference Datasets From the TropiSAR and AfriSAR Campaigns in Support of Upcoming Spaceborne Biomass Missions. IEEE Journal of Selected Topics in Applied Earth Observations and Remote Sensing 11(10), 3617-3627.
- Labrière, N., & Chave, J. (2020a) CCI Biomass project In situ datasets: Processing and validation of Sustainable Landscape Brazil data (CCI Biomass internal report).

esa	Ref	CCI Bio	omass Product Validation Plan v5	
	Issue	Page	Date	
	5.0	35	4-Dec-2024	



- Labrière, N., & Chave, J. (2020b) CCI Biomass project In situ datasets: Processing and validation of NEON data (USA) (CCI Biomass internal report).
- Labrière, N., & Chave, J. (2020c) In situ datasets: Processing and validation of TERN data (CCI Biomass internal report).
- Longo, M., Keller, M., dos-Santos, M. N., Leitold, V., Pinagé, E. R., Baccini, A., ... & Morton, D. C. (2016). Aboveground biomass variability across intact and degraded forests in the Brazilian Amazon. *Global Biogeochemical Cycles*, 30(11), 1639-1660.
- Malone, B.P., McBratney, A.B. and Minasny, B. (2013) Spatial scaling for digital soil mapping. Soil Science Society of America Journal 77(3), 890-902.
- Menlove, J., & Healey, S. P. (2020). A Comprehensive Forest Biomass Dataset for the USA Allows Customized Validation of Remotely Sensed Biomass Estimates. *Remote Sensing*, 12(24), 4141. https://doi.org/10.3390/rs12244141.
- Olofsson, P., Foody, G.M., Herold, M., Stehman, S.V., Woodcock, C.E. and Wulder, M.A. (2014) Good practices for estimating area and assessing accuracy of land change. Remote Sensing of Environment 148, 42-57.
- Ploton, P., Mortier, F., Barbier, N. et al. (2020). A map of African humid tropical forest aboveground biomass derived from management inventories. Sci Data 7, 221.
- Quegan, S. and Ciais, P. (2018) CCI BIOMASS User Requirement Document Year 1
- Réjou-Méchain, M., Barbier, N., Couteron, P., Ploton, P., Vincent, G., Herold, M., Mermoz, S., Saatchi, S., Chave, J., de Boissieu, F., Féret, J.-B., Takoudjou, S.M. and Pélissier, R. (2019) Upscaling Forest Biomass from Field to Satellite Measurements: Sources of Errors and Ways to Reduce Them. Surveys in Geophysics.
- Réjou-Méchain, M., Muller-Landau, H.C., Detto, M., Thomas, S.C., Le Toan, T., Saatchi, S.S., Barreto-Silva, J.S., Bourg, N.A., Bunyavejchewin, S., Butt, N., Brockelman, W.Y., Cao, M., Cárdenas, D., Chiang, J.M., Chuyong, G.B., Clay, K., Condit, R., Dattaraja, H.S., Davies, S.J., Duque, A., Esufali, S., Ewango, C., Fernando, R.H.S., Fletcher, C.D., N. Gunatilleke, I.A.U., Hao, Z., Harms, K.E., Hart, T.B., Hérault, B., Howe, R.W., Hubbell, S.P., Johnson, D.J., Kenfack, D., Larson, A.J., Lin, L., Lin, Y., Lutz, J.A., Makana, J.R., Malhi, Y., Marthews, T.R., McEwan, R.W., McMahon, S.M., McShea, W.J., Muscarella, R., Nathalang, A., Noor, N.S.M., Nytch, C.J., Oliveira, A.A., Phillips, R.P., Pongpattananurak, N., Punchi-Manage, R., Salim, R., Schurman, J., Sukumar, R., Suresh, H.S., Suwanvecho, U., Thomas, D.W., Thompson, J., Uríarte, M., Valencia, R., Vicentini, A., Wolf, A.T., Yap, S., Yuan, Z., Zartman, C.E., Zimmerman, J.K. and Chave, J. (2014) Local spatial structure of forest biomass and its consequences for remote sensing of carbon stocks. Biogeosciences 11(23), 6827-6840.
- Réjou-Méchain, M., Tanguy, A., Piponiot, C., Chave, J. and Hérault, B. (2017) biomass: an r package for estimating above-ground biomass and its uncertainty in tropical forests. Methods in Ecology and Evolution 8(9), 1163-1167.
- Rodríguez-Veiga, P., Quegan, S., Carreiras, J., Persson, H.J., Fransson, J.E.S., Hoscilo, A., Ziółkowski, D., Stereńczak, K., Lohberger, S., Stängel, M., Berninger, A., Siegert, F., Avitabile, V., Herold, M., Mermoz, S., Bouvet, A., Le Toan, T., Carvalhais, N., Santoro, M., Cartus, O., Rauste, Y., Mathieu, R., Asner, G.P., Thiel, C., Pathe, C., Schmullius, C., Seifert, F.M., Tansey, K. and Balzter, H. (2019) Forest biomass retrieval approaches from earth observation in different biomes. International Journal of Applied Earth Observation and Geoinformation 77, 53-68.
- Rozendaal, D.M.A., Santoro, M., Schepaschenko, D., Avitabile, V. and Herold, M. (2017) DUE GlobBiomass D17 Validation Report, p. 26, European Space Agency (ESA-ESRIN).
- Santoro, M., Eriksson, L.E.B. and Fransson, J.E.S. (2015) Reviewing ALOS PALSAR backscatter observations for stem volume retrieval in Swedish forest. Remote Sensing 7(4), 4290-4317.
- Tejada, G., Görgens, E.B., Espírito-Santo, F.D.B., Cantinho, R.Z. and Ometto, J.P. (2019) Evaluating spatial coverage of data on the aboveground biomass in undisturbed forests in the Brazilian Amazon. Carbon Balance and Management 14, pp.1-18. https://doi.org/10.1186/s13021-019-0126-8
- Ulander, L.M.H., Gustavsson, A., Flood, B., Murdin, D., Dubois-Fernandez, P., Dupuis, X., Sandberg, G., Soja, M.J., Eriksson, L.E.B., Fransson, J.E.S., Holmgren, J., Wallerman, J. (2011). BioSAR 2010 Technical assistance for the development of airborne SAR and geophysical measurements during the BioSAR 2010 experiment.
- Wager, S., Hastie, T. and Efron, B. (2014) Confidence intervals for random forests: The jackknife and the infinitesimal jackknife. Journal of Machine Learning Research 15, 1625-1651.
- World Meteorological Organization (2011). Systematic observation requirements for satellite-based data products for climate: Supplemental details to the satellite-based component of the Implementation Plan for the Global

esa	Ref	CCI Bi	omass Product Validation Plan v5
	Issue	Page	Date
	5.0	36	4-Dec-2024



Observing System for Climate in Support of the UNFCCC (2010 Update). $https://library.wmo.int/doc_num.php?explnum_id=3710.$

esa	Ref	CCI Bio	omass Product Validation Plan v5
	Issue	Page	Date
	5.0	37	4-Dec-2024



APPENDIX 1. Plot data used for validating CCI Biomass products.

ID	Tier	Average year	Average size (ha)	Count	Biome	URL	Paper / source	Data access
AFR_L	3	2011	25.00	1	Tropical rainforest	https://dspace.stir.ac.uk/retrieve/74d3b352-fa46-418f-ba95-728bb33f4cfc/08417912.pdf	(Labrière et al., 2018)	open
EU_FOS	3	2014	16.25	1	Tropical rainforest	https://wwwture.com/articles/s41597-019-0196-1?fbclid=IwAR08vLoOm4xEQo4EUdLtoKsnP6nsNIY5CYnfcoqGcS5Z0_UcyaNIr-jcdDg	(Schepaschenko et al., 2019)	open
SAM_L	3	2010	7.65	20	Tropical rainforest	https://dspace.stir.ac.uk/retrieve/74d3b352-fa46-418f-ba95-728bb33f4cfc/08417912.pdf	(Labrière et al., 2018)	open
AUS1	3	2009	25.00	1	Tropical dry forest	http://data.auscover.org.au/xwiki/bin/view/Product+pages/Biomass+Plot+Library	(Paul et al., 2016)	source-WUR agreement
SAM_RF	3	2008	5.3	10	Tropical rainforest	http://www.rainfor.org/en/project/about-rainfor	Lopez-Gonzales et al., 2011	Open
AFR_FOS	2	2013	1.00	44	Tropical rainforest	https://wwwture.com/articles/s41597-019-0196-1?fbclid=IwAR08vLoOm4xEQo4EUdLtoKsnP6nsNIY5CYnfcoqGcS5Z0_UcyaNIr-jcdDg	(Schepaschenko et al., 2019)	open
AFR_L	2	2016	1.00	56	Tropical rainforest	https://dspace.stir.ac.uk/retrieve/74d3b352-fa46-418f-ba95-728bb33f4cfc/08417912.pdf	(Labrière et al., 2018)	open
AUS_FOS	2	2008	1.00	2	Tropical dry forest	https://wwwture.com/articles/s41597-019-0196-1?fbclid=IwAR08vLoOm4xEQo4EUdLtoKsnP6nsNIY5CYnfcoqGcS5Z0_UcyaNIr-jcdDg	(Schepaschenko et al., 2019)	open
CAM_FOS	2	2012	1.01	18	Tropical rainforest	https://wwwture.com/articles/s41597-019-0196-1?fbclid=IwAR08vLoOm4xEQo4EUdLtoKsnP6nsNIY5CYnfcoqGcS5Z0_UcyaNIr-jcdDg	(Schepaschenko et al., 2019)	open
EU_FOS	2	2010	2.23	2	Boreal coniferous forest	https://wwwture.com/articles/s41597-019-0196-1?fbclid=IwAR08vLoOm4xEQo4EUdLtoKsnP6nsNIY5CYnfcoqGcS5Z0_UcyaNIr-jcdDg	(Schepaschenko et al., 2019)	open
SAM_FOS	2	2011	1.00	23	Tropical rainforest	https://wwwture.com/articles/s41597-019-0196-1?fbclid=IwAR08vLoOm4xEQo4EUdLtoKsnP6nsNIY5CYnfcoqGcS5Z0_UcyaNIr-jcdDg	(Schepaschenko et al., 2019)	open
SAM_L	2	2013	1.04	28	Tropical rainforest	https://dspace.stir.ac.uk/retrieve/74d3b352-fa46-418f-ba95-728bb33f4cfc/08417912.pdf	(Labrière et al., 2018)	open
SAM_BAJ	2	2017	1	3	Tropical rainforest	https://ieeexplore.ieee.org/abstract/document/8518871	Pacheco- Pasccagaza et al., 2020	source-WUR agreement
SAM_RF	2	2008	1	374	Tropical rainforest	http://www.rainfor.org/en/project/about-rainfor	Lopez-Gonzales et al., 2011	Open

	Ref	CCI Bio	omass Product Validation Plan v5
esa	Issue	Page	Date
	5.0	38	4-Dec-2024



	1	ı	1	1	T		1	
UK_FOS	2	2015	1.20	1	Tropical rainforest	https://wwwture.com/articles/s41597-019-0196- 1?fbclid=IwAR08vLoOm4xEQo4EUdLtoKsnP6nsNIY5CYnfcoqGcS5Z0_UcyaNIr-jcdDg	(Schepaschenko et al., 2019)	open
AFR10	2	2007	1.00	7	Tropical rainforest	https://iopscience.iop.org/article/10.1088/1748-9326/6/4/049001/meta	(Mitchard et al., 2011)	source-WUR agreement
AFR13	2	2008	1.00	2	Tropical rainforest	https://agupubs.onlinelibrary.wiley.com/doi/full/10.1029/2009GL040692	(Mitchard et al., 2009)	source-WUR agreement
AFR14	2	2009	1.63	4	Tropical rainforest	https://www.sciencedirect.com/science/article/abs/pii/S014362281400109X	(Ryan, Berry, & Joshi, 2014)	source-WUR agreement
AFR6	2	2009	1.00	12	Tropical rainforest	https://cbmjour-l.biomedcentral.com/articles/10.1186/1750-0680-9-2	(Willcock et al., 2014)	source-WUR agreement
AFR7	2	2012	1.00	19	Tropical rainforest	https://royalsocietypublishing.org/doi/full/10.1098/rstb.2012.0295	(Lewis et al., 2013)	source-WUR agreement
ASI3	2	2007	1.00	92	Tropical rainforest	https://www.sciencedirect.com/science/article/abs/pii/S0378112711004361	(Morel et al., 2011)	source-WUR agreement
AUS1	2	2012	1.01	63	Subtropical steppe	http://data.auscover.org.au/xwiki/bin/view/Product+pages/Biomass+Plot+Library	(Paul et al., 2016)	source-WUR agreement
SAM2	2	2012	1.00	40	Tropical rainforest	http://geoinfo.cnpm.embrapa.br/geonetwork/srv/ eng/main.home		source-WUR agreement
SAM_FOS	1	2011	0.25	142	Tropical rainforest	https://wwwture.com/articles/s41597-019-0196-1?fbclid=IwAR08vLoOm4xEQo4EUdLtoKsnP6nsNIY5CYnfcoqGcS5Z0_UcyaNIr-jcdDg	(Schepaschenko et al., 2019)	open
AFR15	1	2013	0.25	136	Tropical rainforest	https://besjour-ls.onlinelibrary.wiley.com/doi/full/10.1111/1365- 2745.12548%4010.1111/%28ISSN%291365-2745.FORESTRY	(Vieilledent et al., 2016)	source-WUR agreement
AFR1	1	2008	0.50	1152	Tropical rainforest	https://agritrop.cirad.fr/572060/1/document_572060.pdf	(Hirsh, Jourget, Feintrenie, Bayol, & Ebaá Atyi, 2013)	source-WUR agreement
AFR10	1	2007	0.50	11	Tropical rainforest	https://iopscience.iop.org/article/10.1088/1748-9326/6/4/049001/meta	(Mitchard et al., 2011)	source-WUR agreement
AFR12	1	2008	0.16	108	Tropical rainforest	https://www.sciencedirect.com/science/article/abs/pii/S0034425711003609	(Avitabile, Baccini, Friedl, & Schmullius, 2012)	source-WUR agreement
AFR13	1	2008	0.50	23	Tropical rainforest	https://agupubs.onlinelibrary.wiley.com/doi/full/10.1029/2009GL040692	(Mitchard et al., 2009)	source-WUR agreement
AFR14	1	2009	0.51	70	Tropical dry forest	https://www.sciencedirect.com/science/article/abs/pii/S014362281400109X	(Ryan et al., 2014)	source-WUR agreement
AFR4	1	2012	0.13	110	Tropical mountain system	http://www.geo-informatie.nl/workshops/scw2/papers/deVries.pdf	(DeVries, Avitabile, Kooistra, & Herold, 2012)	source-WUR agreement

	Ref	CCI Bio	omass Product Validation Plan v5
esa	Issue	Page	Date
	5.0	39	4-Dec-2024



AFR5	1	2012	0.08	71	Tropical rainforest	https://pure.mpg.de/pubman/faces/ViewItemOverviewPage.jsp?itemId=item_2281402	(Vaglio Laurin et al., 2016)	source-WUR agreement
AFR6	1	2009	0.33	12	Tropical dry forest	https://cbmjour-l.biomedcentral.com/articles/10.1186/1750-0680-9-2	(Willcock et al., 2014)	source-WUR agreement
AFR8	1	2008	0.13	105	Tropical moist forest	https://www.sciencedirect.com/science/article/abs/pii/S0034425712001058	(Carreiras, Vasconcelos, & Lucas, 2012)	source-WUR agreement
AFR9	1	2016	0.13	9642	Tropical dry forest	https://www.mdpi.com/2072-4292/5/4/1524 https://fndsmoz.maps.arcgis.com/apps/MapSeries/index.html?appid=6602939f39ad4626a10f87bf625 3af1e	(Carreiras et al., 2012)	open, source- WUR agreement
AFR_KEN	1	2011	0.09	362	Tropical and subtropical grasslands, savannas and shrublands			source-WUR agreement
ASI1	1	2008	0.05	2903	Tropical mountain system and rainforest	https://www.tandfonline.com/doi/full/10.1080/17583004.2016.1254009	(Avitabile et al., 2016)	source-WUR agreement
ASI10	1	2008	0.10	1268	Subtropical mountain system	https://www.sciencedirect.com/science/article/abs/pii/S0034425719303608	Zhang et al. 2019	source-WUR agreement
ASI2	1	2011	0.11	119	Tropical dry forest	http://www.leafasia.org/sites/default/files/public/resources/WWF-REDD-pres-July-2013-v3.pdf	WWF and OBf, 2013	source-WUR agreement
ASI4	1	2010	0.02	70	Tropical dry forest	http://citeseerx.ist.psu.edu/viewdoc/download?doi=10.1.1.972.708&rep=rep1&type=pdf	Wijaya et al., 2015	source-WUR agreement
ASI9	1	2012	0.13	74	Tropical rainforest	http://leutra.geogr.uni-jede/vgtbRBIS/metadata/start.php	Avitabile et al., 2014	source-WUR agreement
ASI_FOS	1	2014	0.25	2	Tropical rainforest	https://wwwture.com/articles/s41597-019-0196-1?fbclid=IwAR08vLoOm4xEQo4EUdLtoKsnP6nsNIY5CYnfcoqGcS5Z0_UcyaNIr-jcdDg	(Schepaschenko et al., 2019)	open
AUS1	1	2011	0.12	5611	Tropical dry forest	http://data.auscover.org.au/xwiki/bin/view/Product+pages/Biomass+Plot+Library	Paul et al. 2016	source-WUR agreement
EU1	1	2011	0.01	16819	Temperate broadleaf and mixed forests and Boreal forests	https://www.slu.se/en/collaborative-centres-and-projects/swedishtio-l-forest-inventory/	Sweden NFI	source-WUR agreement
EU2	1	2007	0.20	7177	Mediterranean forests	http://www.magrama.gob.es/es/desarrollo-rural/temas/politica-forestal/inventario-cartografia/inventario-forestalcio-l/	Spain NFI	source-WUR agreement
EU3	1	2013	0.06	3021	Temperate oceanic forest	https://library.wur.nl/WebQuery/wurpubs/454875	Netherlands NFI	source-WUR agreement
EU4	1	2007	0.06	5967	Temperate broadleaf and mixed forests and Mediterranean forests	https://www.agriculturejour-ls.cz/publicFiles/01003.pdf	Cienciela et al. 2008	source-WUR agreement

	Ref	CCI Bio	omass Product Validation Plan v5
esa	Issue	Page	Date
	5.0	40	4-Dec-2024



EU_FOS	1	2015	0.28	514	Boreal forests	https://wwwture.com/articles/s41597-019-0196-1?fbclid=IwAR08vLoOm4xEQo4EUdLtoKsnP6nsNIY5CYnfcoqGcS5Z0_UcyaNIr-jcdDg	(Schepaschenko et al., 2019)	open, source- WUR agreement
NAM1	1	2010	0.04	586	Boreal coniferous forest	https://www.p-s.org/content/112/18/5738.short	(Liang et al., 2015)	source-WUR agreement
NAM2	1	2004	0.04	75	Temperate mountain system	https://www.nature.com/articles/nature07276	(Luyssaert et al., 2008)	source-WUR agreement
NAM3	1	2010	0.03	588	Temperate continental forest			source-WUR agreement
NAM4	1	2010	0.04	2794	Temperate mountain system		Alaska NFI	source-WUR agreement
SAM2	1	2013	0.23	241	Tropical rainforest	https://www.paisagenslidar.cnptia.embrapa.br/webgis/	Embrapa, undated	source-WUR agreement
SAM3	1	2011	0.13	111	Tropical rainforest		CIFOR, undated	source-WUR agreement
SAM4	1	2014	0.15	7	Tropical rainforest		CIFOR, undated	source-WUR agreement
SAM5	1	2014	0.60	23	Tropical rainforest		CIFOR, undated	source-WUR agreement
SAM_BAJ	1	2017	0.25	363	Tropical rainforest	https://ieeexplore.ieee.org/abstract/document/8518871	(Pacheco- Pasccagaza et al., 2020)	source-WUR agreement
SAM_RF	1	2008	1	125	Tropical rainforest	http://www.rainfor.org/en/project/about-rainfor	(Lopez-Gonzales et al., 2011)	open
SAM_TAPA	1	2009	0.5	138	Tropical rainforest	https://www.tandfonline.com/doi/full/10.1080/07038992.2014.913477?casa_token=EZx eZoegekkAAAAA%3AZHCN98XtpZRrsS9KoGTBhPy1_yzhAkkLZHfck3fomwSnvSa O7YDiuPV_hne6Mj1Wdn-7ME_sPChP	(Bispo et al., 2014)	source-WUR agreement
AFR_COF	0	2009	100	35029	Tropical moist forest,	https://www.nature.com/articles/s41597-020-0561-0	(Ploton et al., 2020)	open
LiDAR	0	2014	1	744397	Tropical rainforest		SLB, TERN, NEON	open
ASI_IR	1	2019	0.16	223	Temperate broadleaf and mixed forests and Mediterranean forests	https://afrjournal.org/index.php/afr/article/view/2390	(Moradi et al., 2021)	source_WUR agreement
EU_WLS	1	2016	0.5	1711	Temperate oceanic forest	https://www.forestresearch.gov.uk/	Wales NFI	MAAP

Ref Issue 5.0	CCI Bio	CCI Biomass Product Validation Plan v5				
esa	Issue	Page	Date			
	5.0	41	4-Dec-2024			



ASI_JAP1	1	2018	1	94	Subtropical mountain system	JAXA / Ministry of Environment Japan (only 0.1 plot-map aggregates are provided)	Japan research plots	MAAP
ASI_JAP2	2	2018	0.1	13000	Subtropical mountain system	JAXA / Japan Forestry Agency (only 0.1 plot-map aggregates are provided)	Japan NFI	MAAP
LVIS	1	2016	1	10000+	Tropical rainforest	https://daac.oml.gov/cgi-bin/dsviewer.pl?ds_id=1775	Armston et al., 2020	MAAP

	Ref	CCI Bio	omass Product Validation Plan v5
esa	Issue	Page	Date
	5.0	42	4-Dec-2024



APPENDIX 2. Reference data potentially useful used for validating and comparing Biomass change products.

Country	Data type	Dominant forest type	Measurement (n)	n	Inventory year	Original size (ha)	AGB change (Mg/ha)	SD estimate	Eco-region	Reference
Netherlands	NFI	Plantation	3	1562	2007-2016	0.04	11.8	no	Temperate broadleaf and mixed forests	Schelhaas et al., 2018
Belgium	NFI	Plantation	3	668	2003-2009	0.1	-2.8	no	Temperate broadleaf and mixed forests	Schelhaas et al., 2018
Sweden	NFI	Plantation	3	12887	2008-2013	0.03	4.9	no	Temperate broadleaf and Boreal forests	Schelhaas et al., 2018
Philippines	NFI	Natural	2	587	2003-2014	0.5	2.8	yes	Tropical rainforest	Araza et al., 2021
Poland	LiDAR	Plantation	2	770	2005- 2019	1	6.5	no	Temperate broadleaf and mixed forests and Boreal forests	Laurin et al., 2020
Czech Republic	LiDAR	Plantation	2	75	2014-2020	0.05	2	yes	Temperate conifer forests	Brovkina et al., 2017
Spain	LiDAR	Plantation	2	54058	2010-2016	0.1	0.86	yes	Mediterranean forests	Mariano et al., under preparation
Bulgaria	LiDAR	Plantation	2	1946	2006-2016	0.1	0.12	yes	Temperate conifer forests	Dmitrov et al., under preparation
Costa Rica	LiDAR	Natural	2	9342	2010-2018	0.1	-0.6	no	Tropical rainforest	Cushman et al. 2021
Brazil	LiDAR	Natural	2	28607	2011-2018	0.1	-17.8	no	Tropical rainforest	Longo et al., 2016
USA	LiDAR	Natural	2	110939	2013-2019	0.1	1.76	no	Temperate broadleaf and Boreal forests	Johnson et al., 2010
Alaska	LiDAR	Natural	2	48552	2013-2019	0.1	1.76	yes	Boreal forest	Johnson et al., 2010